残されたブラックホール観測の課題

根來　均（日大理工）

約 20 年間のトラペからの抜粋

解明すべき BH 物理

High Frequency QPO
Black Hole Spin !?
Remillard et al. 02

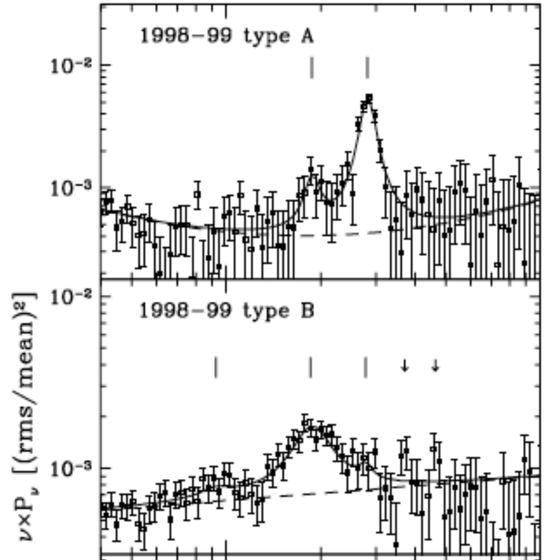

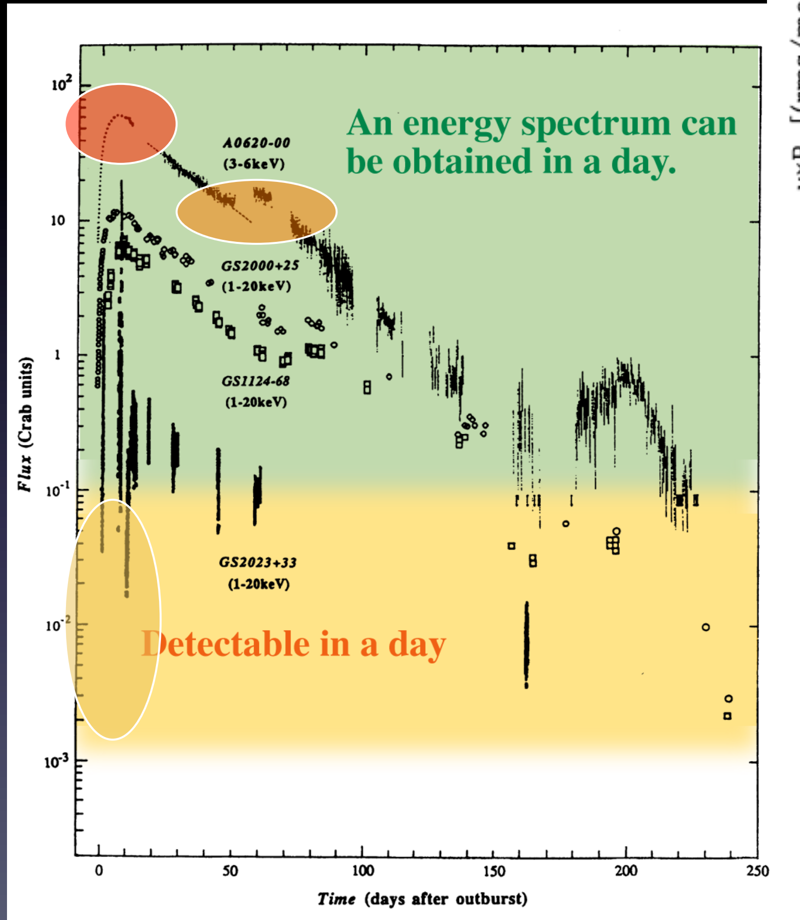

Optical Jet

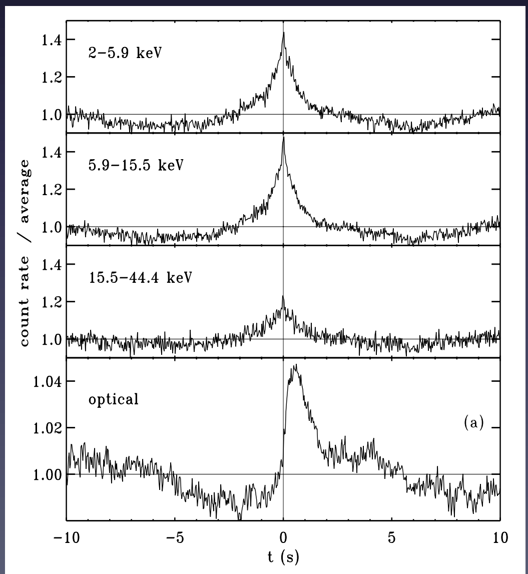

XTE J1118+480 (Malzac+ 2003)

Relativistic Jet

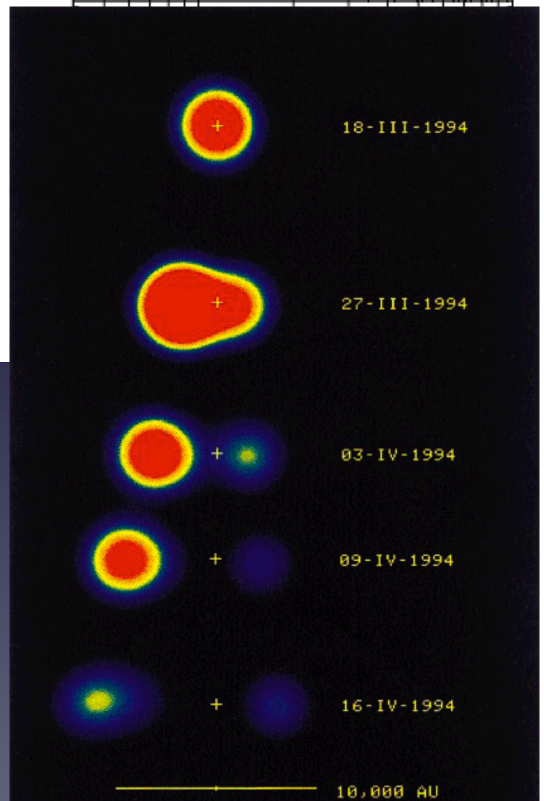

Mirabel et al. 98

MAXI discovered 17 X-ray Novae in 6 years

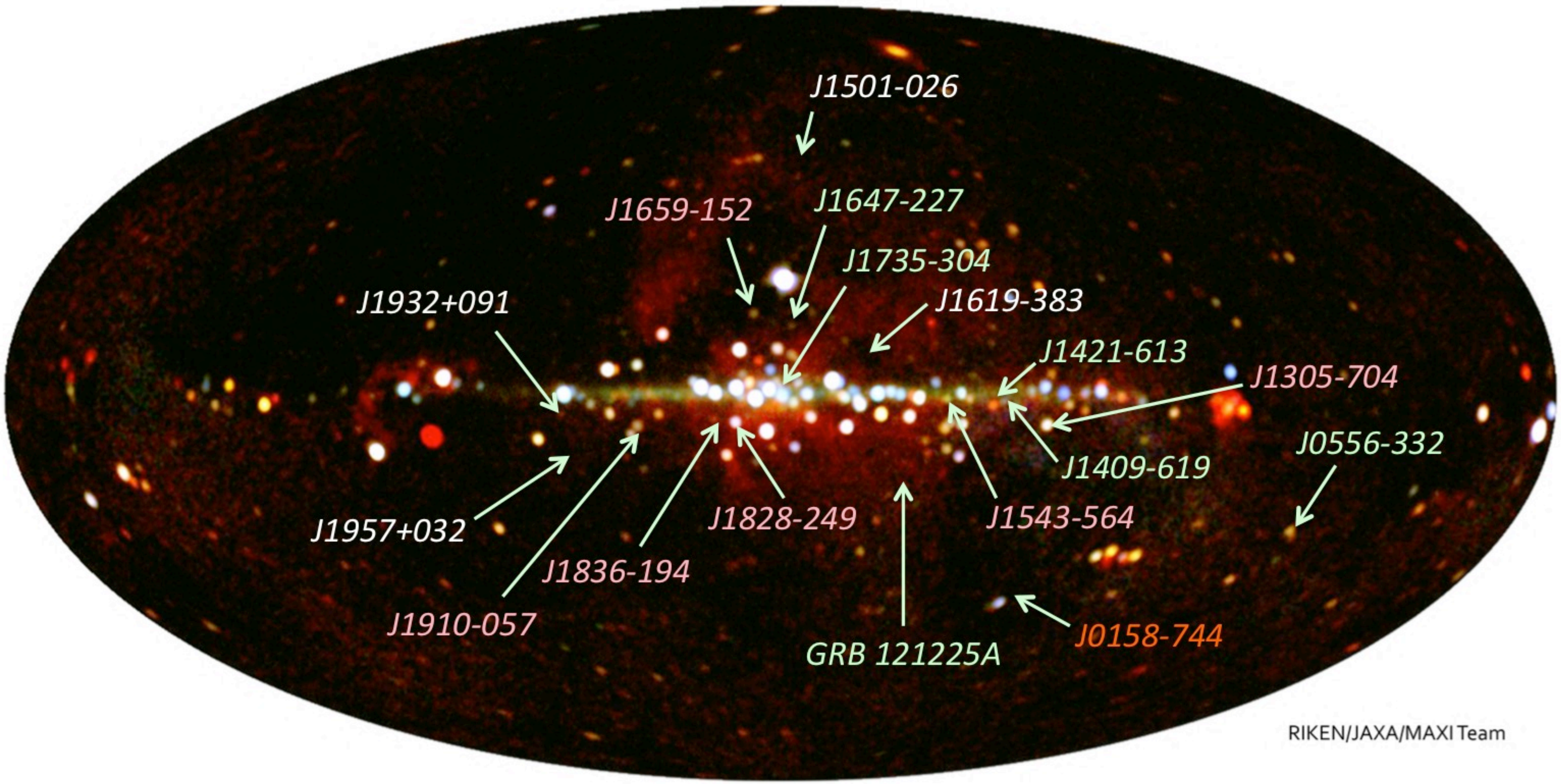

1 White Dwarf, 6 Neutron Stars, 6 Black Hole Candidates, and 4 unknowns

Table A.1. Astrometric properties.

(1) Year	(2) Name	(3) RA (h m s)	(4) Dec (° ′ ″)	(5) Error† ″/(s, ″)	(6) ℓ (°)	(7) b (°)	(8) d (kpc)	(9) z (kpc)	(10) Outb.	(11) Ref.
2014	IGR J17454-2919[1]	17 45 27.69	−29 19 53.83	x 0.6	359.6444	−00.1765				Chenevez et al. (2014a), Paizis et al. (2015)
	IGR J17451-3022[2]	17 45 06.72	−30 22 43.30	x 0.6	358.7115	−00.6580				Chenevez et al. (2014c), Chakrabarty et al. (2014)
2013	MAXI J1828-249	18 28 58.07	−25 01 45.88	o 0.03	008.1145	−06.5458				Nakahira et al. (2013), Kennea et al. (2013)
	SWIFT J1753.7-2544	17 53 39.85	−25 45 14.20	i 0.3	003.6476	+00.1036				Krimm et al. (2013), Rau et al. (2013a)
2012	SWIFT J174510.8-262411	17 45 10.85	−26 24 12.60	r (0.001,0.01)	002.1107	+01.4034	<7*	<0.17		Cummings et al. (2012), Miller-Jones & Sivakoff (2012) Muñoz-Darias et al. (2013)
	SWIFT J1910.2-0546 (MAXI J1910-057)	19 10 22.80	−05 47 55.92	o 0.3	029.9026	−06.8440				Krimm et al. (2012), Usui et al. (2012), Rau et al. (2012)
	MAXI J1305-704	13 06 55.30	−70 27 05.11	r (0.003,0.07)	304.2375	−07.6177				Sato et al. (2012), Coriat et al. (2012)
2011	MAXI J1836-194[3]	18 35 43.44	−19 19 10.48	e (0.000003 ,0.0002)	013.9456	−05.3542	7 ± 3	−0.70 ± 0.30		Negoro et al. (2011b), Russell et al. (2014, 2015)
	MAXI J1543-564[4]	15 43 17.18	−56 24 49.61	r (0.049,0.775)	325.0855	−01.1214				Negoro et al. (2011a), Miller-Jones et al. (2011b)
	SWIFT J1357.2-0933[5]	**13 57 16.82**	**−09 32 38.55**	**oi 0.3**	**328.7019**	**+50.0042**	**>2.29**	**>1.75**		**Krimm et al. (2011b), Rau et al. (2011b), Mata Sánchez et al. (2015)**
2010	MAXI J1659-152	16 59 01.68	−15 15 28.73	e 0.0001	005.5003	+16.5167	8.60 ± 3.70	2.44 ± 1.05		Negoro et al. (2010), Paragi et al. (2010), Kuulkers et al. (2013)
2009	XTE J1752-223	17 52 15.09	−22 20 32.36	e 0.0014	006.4231	+02.1143	6 ± 2	0.22 ± 0.07		Markwardt et al. (2009b), Miller-Jones et al. (2011a), Ratti et al. (2012)
	XTE J1652-453[6]	16 52 20.33	−45 20 39.99	r 0.32	340.5297	−00.7867				Markwardt et al. (2009c), Calvelo et al. (2009a)

Corral-Santana+ 2016

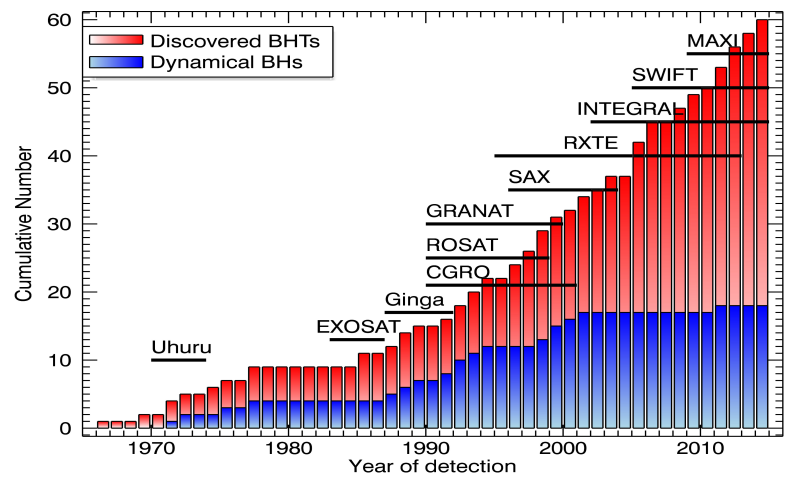

Fig. 1. Cumulative histogram of discovered (red) and dynamically confirmed (blue) BHTs as a function of time. Here, we also count *Swift* J1357.2−0933 as a dynamical BH. The lifetimes of the main X-ray satellites with all-sky monitor capabilities are shown with black lines.

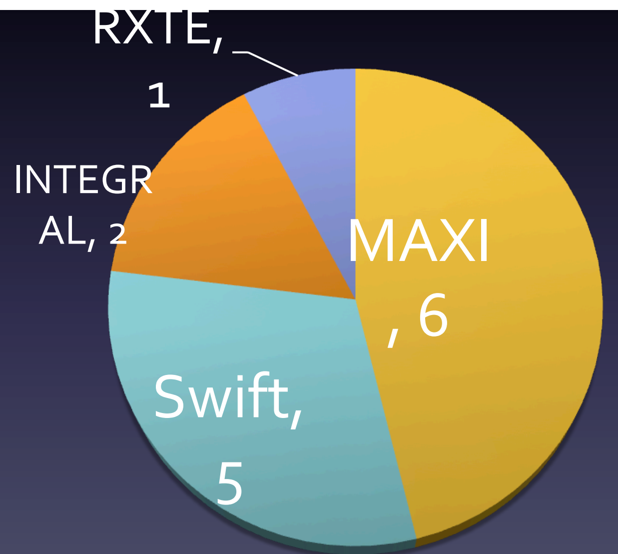

ASM: MAXI, Swift/BAT, INTEGRAL

+ Pointing Sat:

Swift/XRT

ASTROSAT (2015/10~) (~RXTE)

Hitomi (2016/02~)

State (状態)

Low/Hard State

激しい

短時間変動

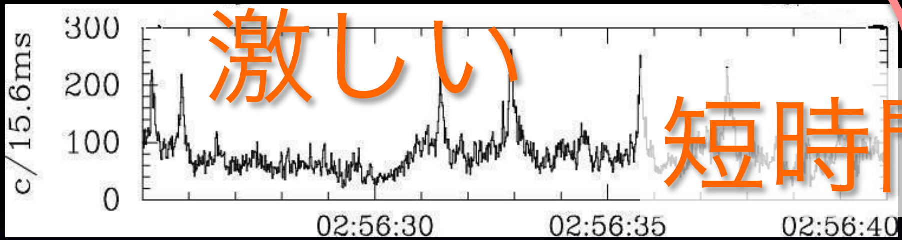

Cyg X-1:
Negoro 1995

べき状

$E^{-\alpha} \exp(-E/E_c)$

エネルギー
スペクトル

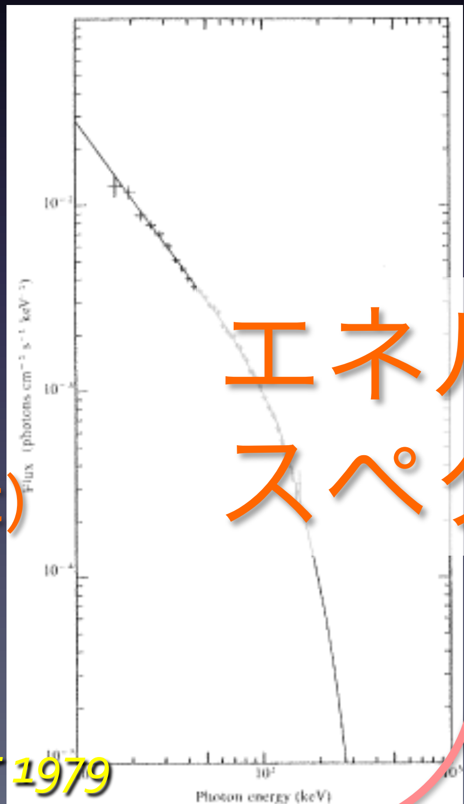

Cyg X-1:
Sunyaev & Trumper 1979

High/Soft State

穏やか

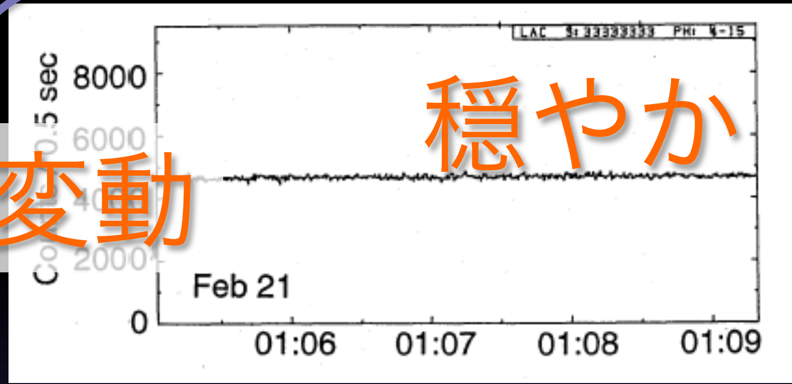

GS 1124-68: *Ebisawa et al. 1994*

熱的成分＋
ハードテイル

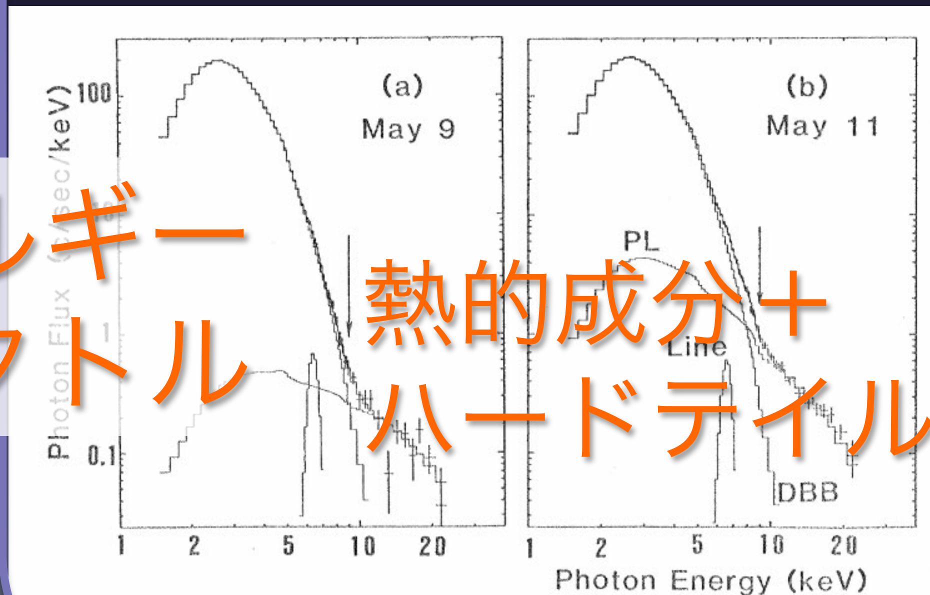

GX339-4: *Makishima et al. 1986*

Observations vs Theories

- Low/Hard State
  - Power-Law (= Advection Flow, Corona or jet ?)
  - Flickering (= Advection)
- Intermediate State
  - Steep Power-Law dominant (= Corona Dominant Disk ?)
  - QPOs (=inner boundary instability, disk warp, Lense-Thirring ??)
- High/Soft State
  - Thermal Disk (= S-S Standard Disk) + Power-Law tail (= Corona ?)

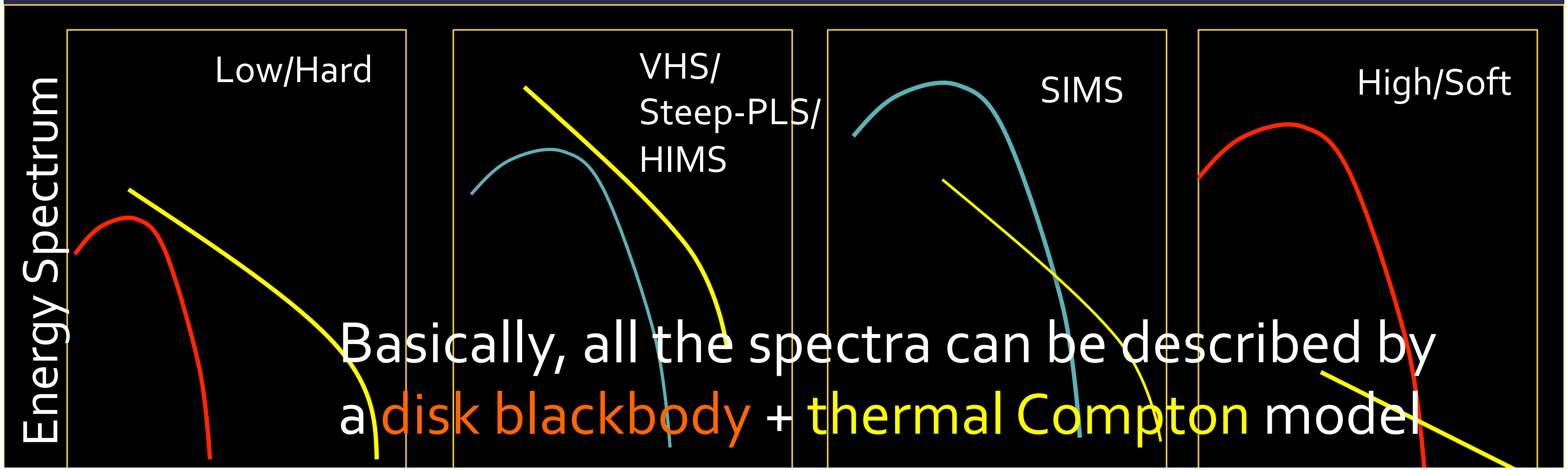

Basically, all the spectra can be described by a disk blackbody + thermal Compton model

様々な時間変動

Cyg X-1 ***HS***: *Negoro 1995*

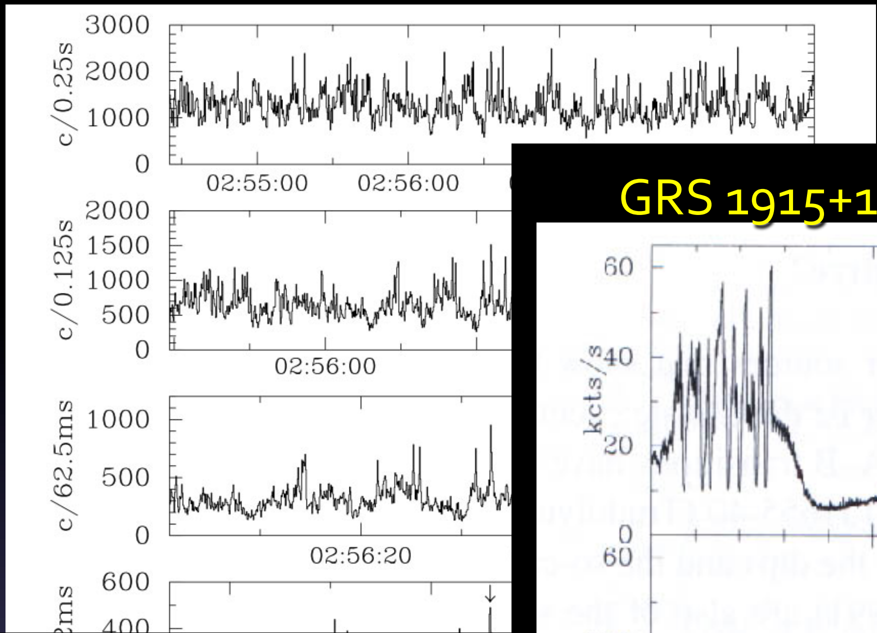

GS 1124-68 ***SS***: *Ebisawa et al. 1994*

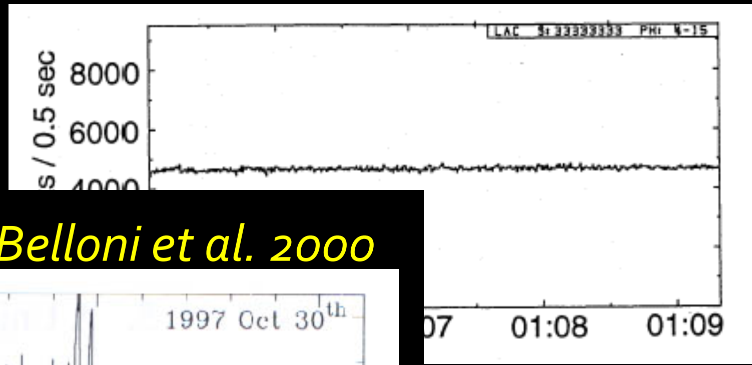

GRS 1915+105 ?: *Belloni et al. 2000*

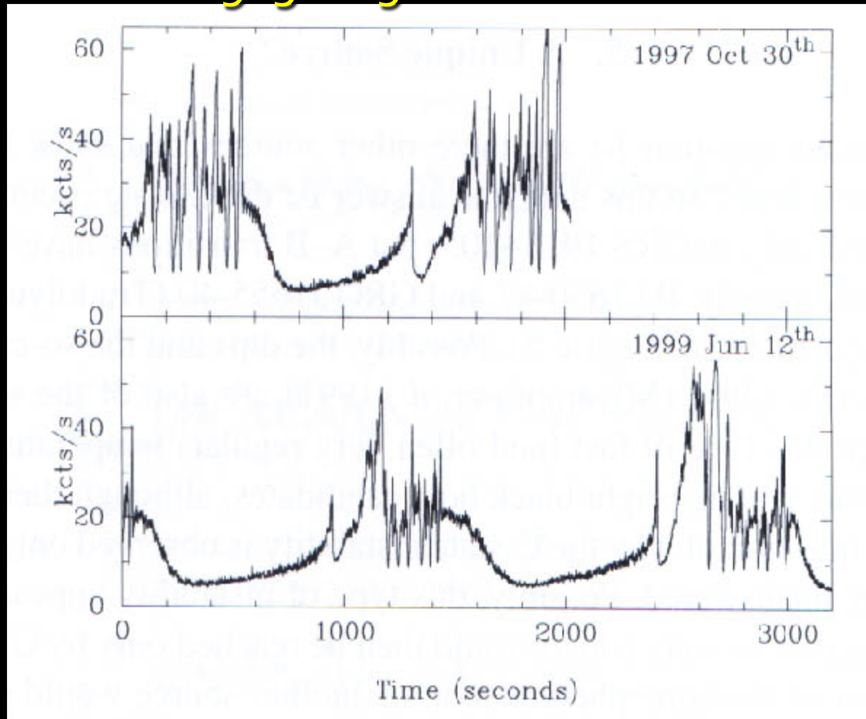

XTE J1550+564 **VHS(IMS**

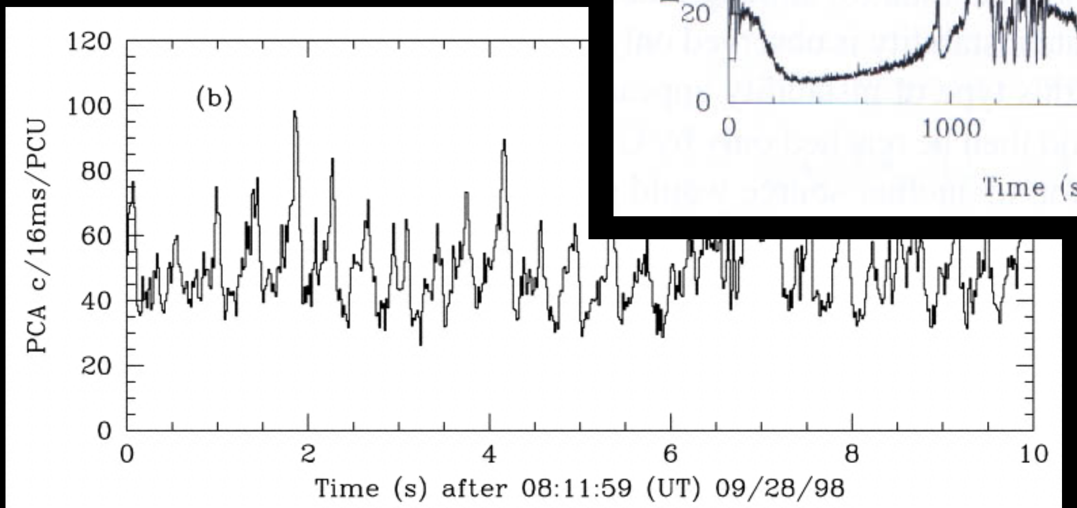

GX 339-4 ***VHS*** : *Miyamoto et al. 1991*

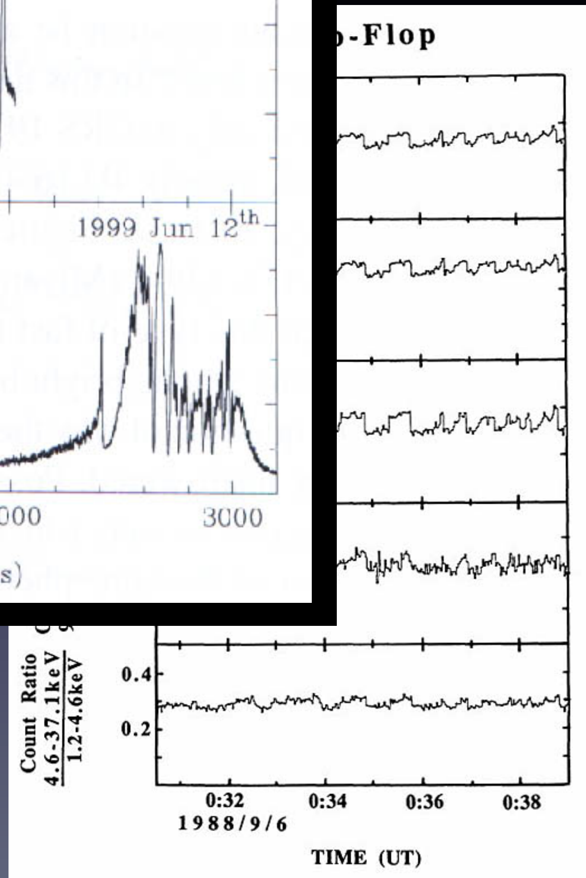

Hard State

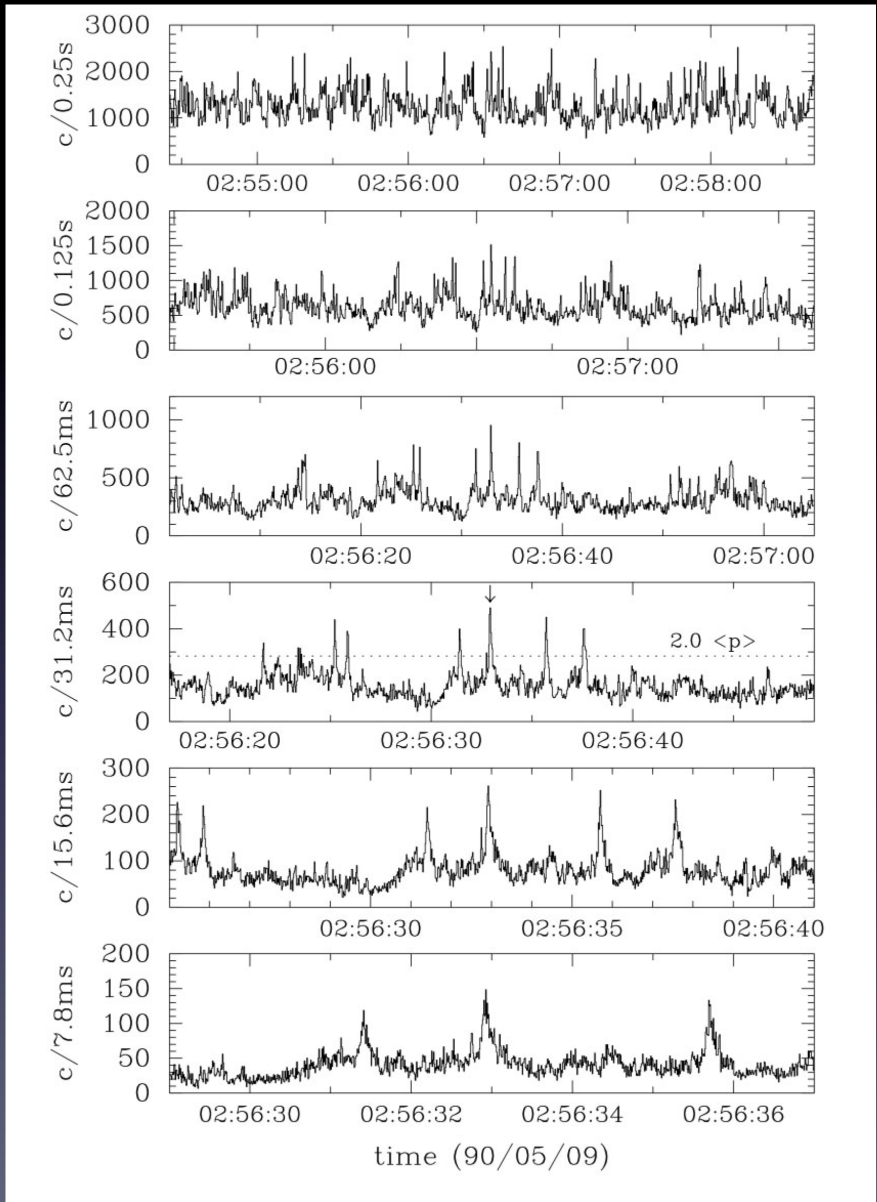

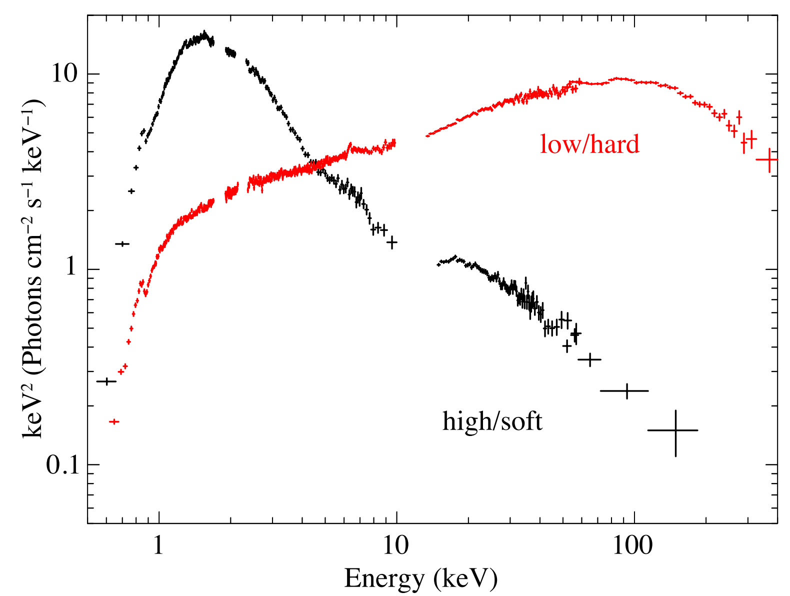

Fig. 1. Suzaku spectra of Cyg X-1 in the response-removed νF_ν form. The black one was obtained in the high/soft state on 2010 December 16. The red one was taken in the low/hard state on 2005 October 5, which is the same as used in Paper I. (Color online)

Yamada+ 2013

Rapid Variation, Shot - *Density Fluctuation on ADAF*

Cyg X-1 (Ginga) Negoro+ 1994, Negoro 1995

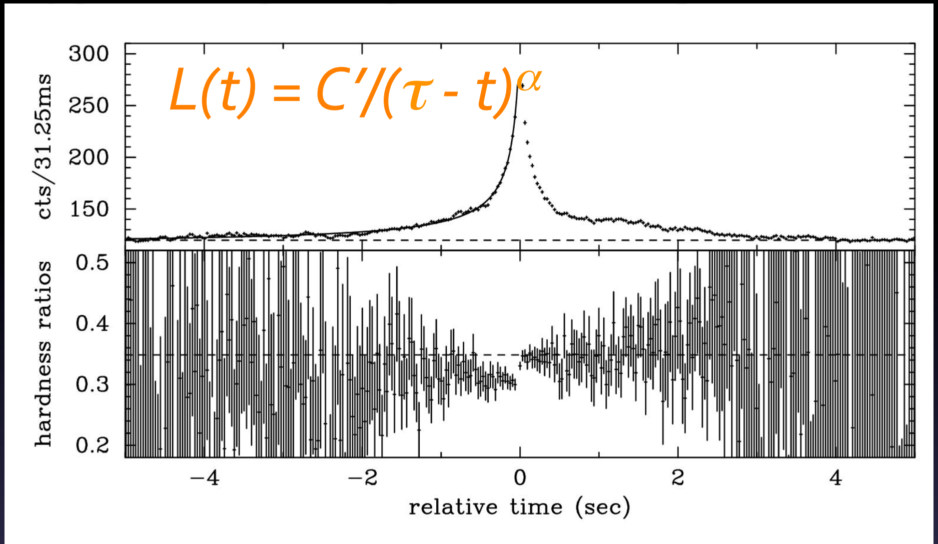

radial velocity

$$dr/dt = - C\, r^{-1/2}$$

released energy

$$L = GMm/2r^2\ (-dr/dt)$$

"Propagating model"
Also see Kotov+ 2001.

Manmoto+ 1996

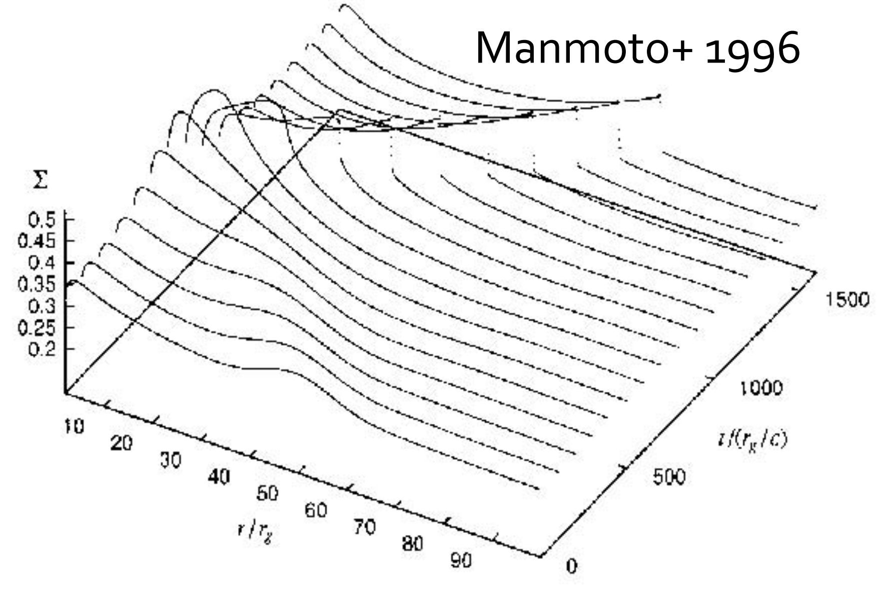

Machida+2002

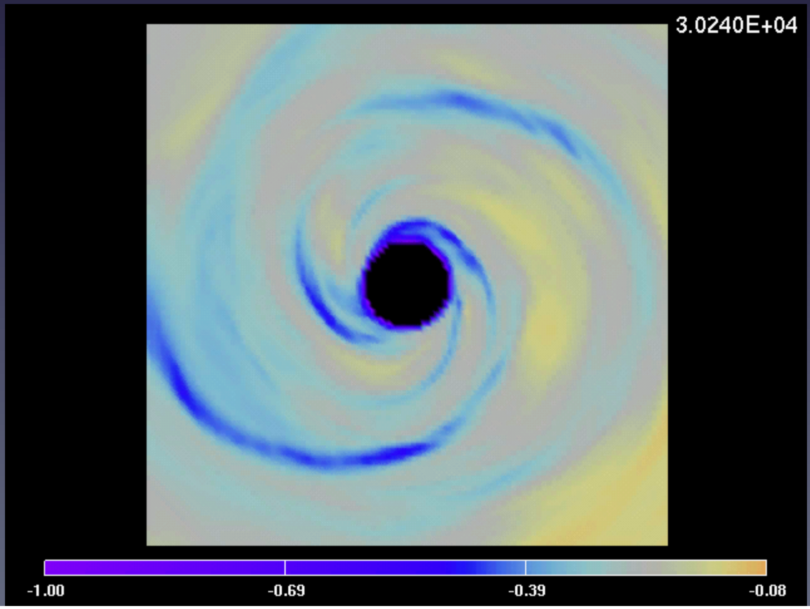

Makishima+ 2008 (Suzaku)

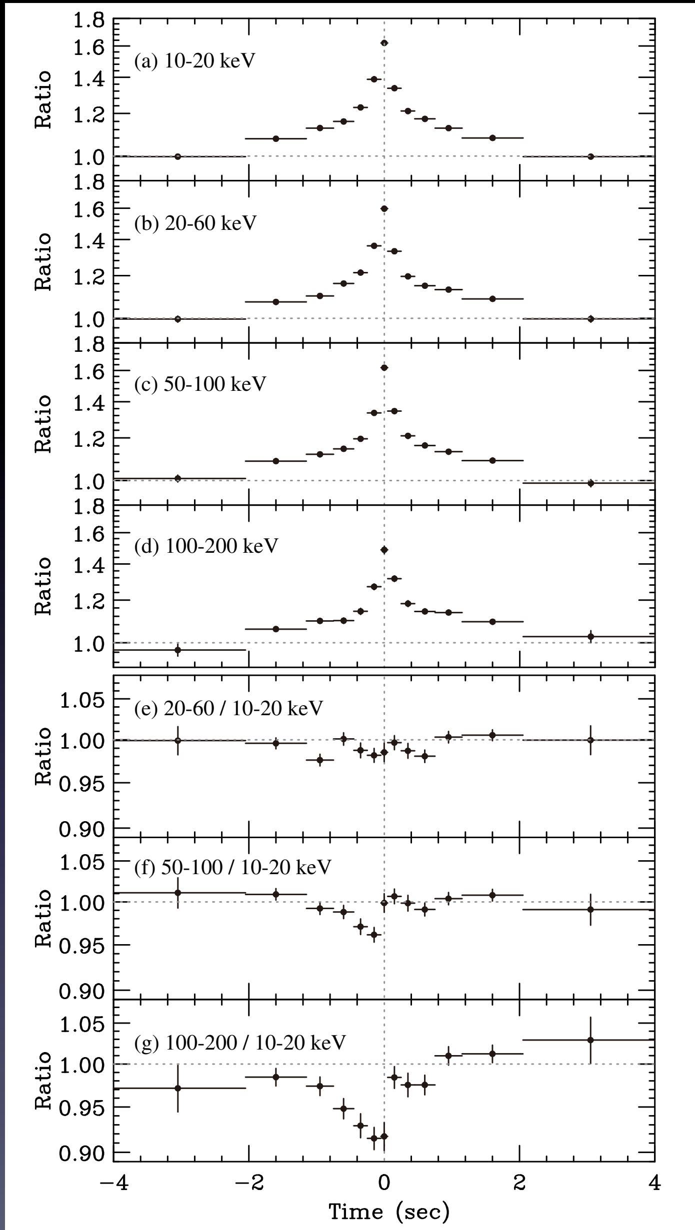

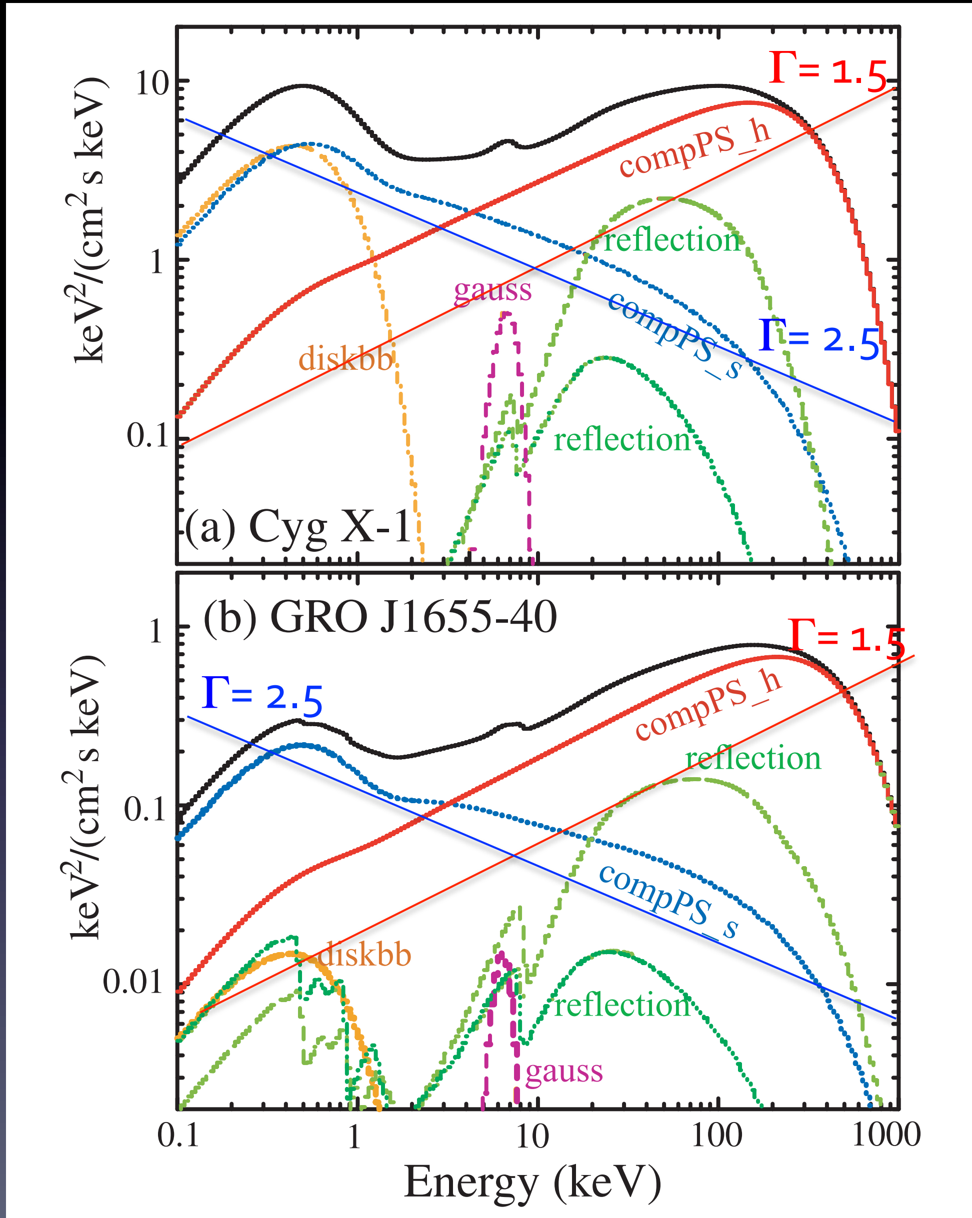

Cyg X-1 (Suzaku) Yamada+ 2013

ブラックホール近傍でジェットの発生？

XTE J1118+480 CCF of X-rays & Optical
Kanbach et al., 2001 Nature, 414, 180

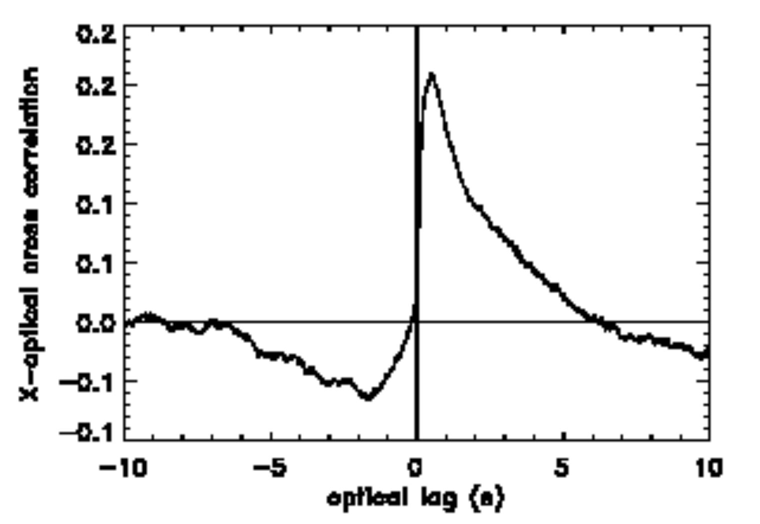

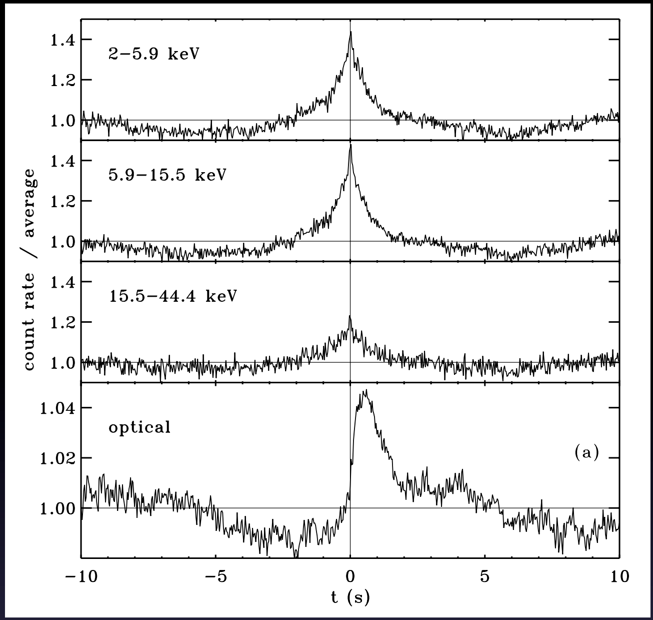

XTE J1118+480 (Malzac+ 2003)
also GX 339-4 (Gandhi+ 2010)

Spruit & Kanbach, 2002 A&A, 391, 225

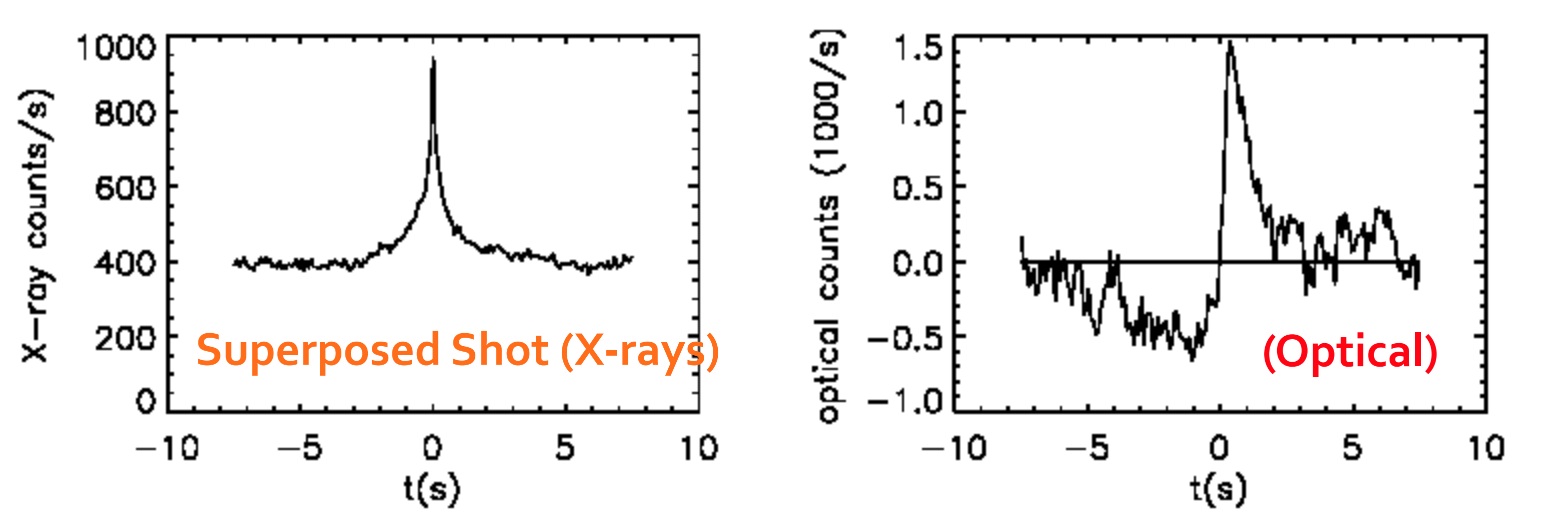

ショットの発生:
ジェットへのエネルギー供給

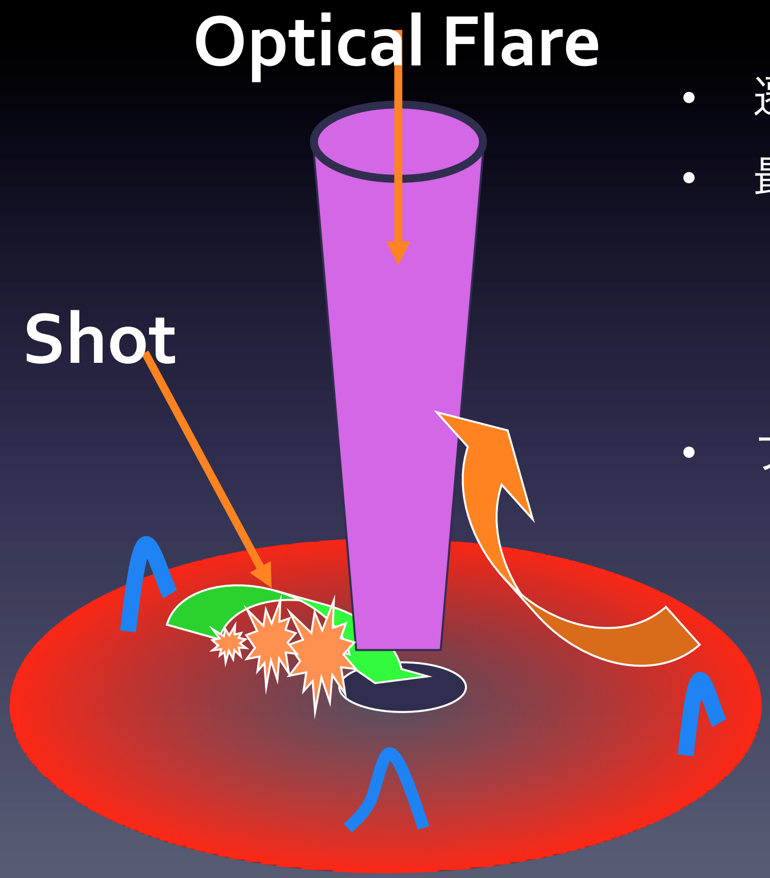

- 遷音速流でのショック
- 最内縁付近での磁気再結合/圧縮
  - e.g., Machida+ 2002, Kato+ 2004 (磁気タワー)
  - 磁気遠心力加速モデル (Blandford & Payne 1982 ~) では説明が厳しい？
- ブラックホールの回転のエネルギーの抜き取り（ペンローズ過程）

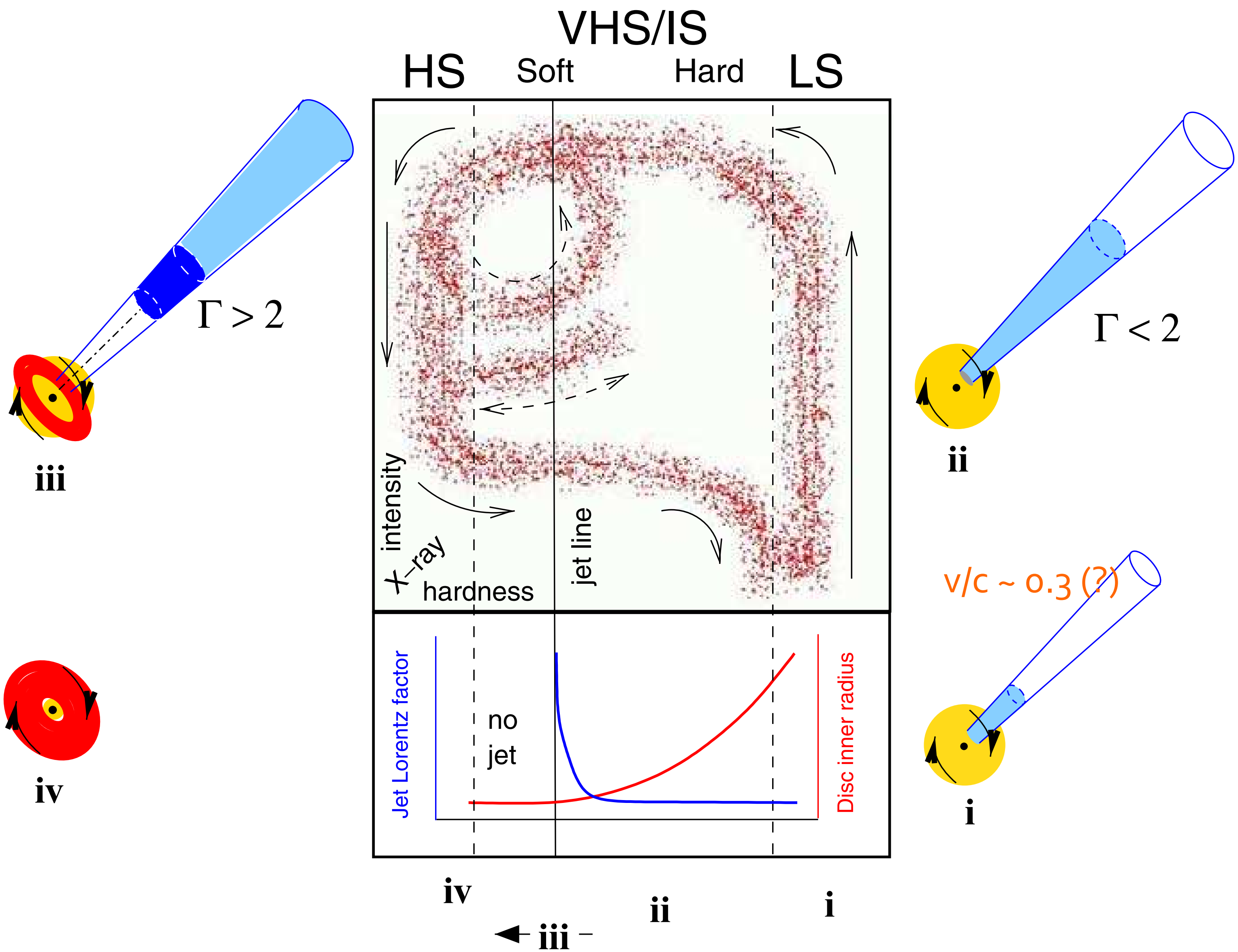

VHS/IS
HS
Soft
Hard
LS
Γ > 2
Γ < 2
iii
ii
iv
i
v/c ~ 0.3 (?)
X–ray intensity
hardness
jet line
Jet Lorentz factor
no jet
Disc inner radius
iv
ii
i
iii

Fender+ 2004

Jet as the origin of the PL?

e.g., Markoff+2001

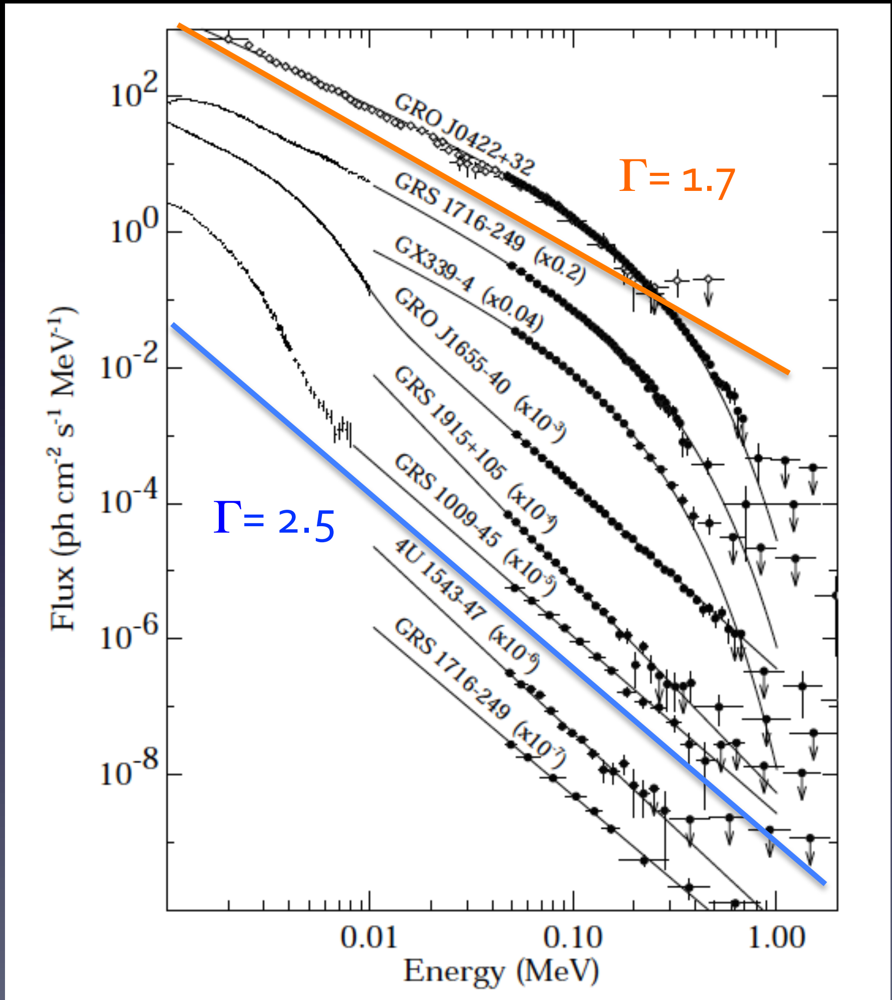

Grove+ 1998

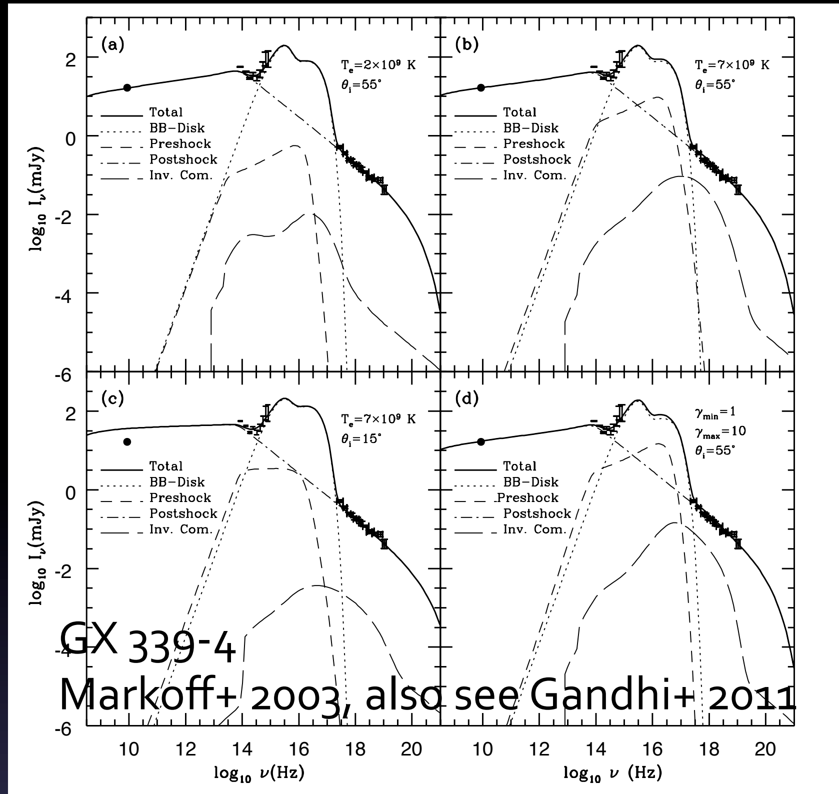

GX 339-4
Markoff+ 2003, also see Gandhi+ 2011

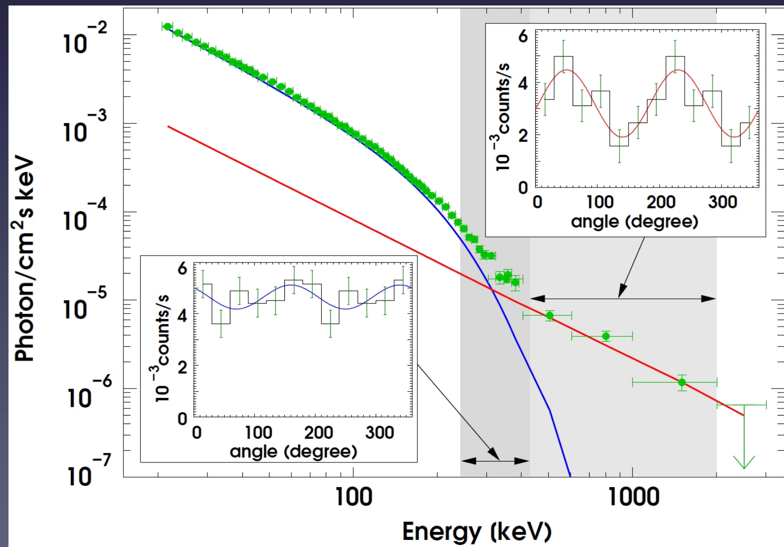

Cyg X-1 (Laurent+ 2011, Rodriguez+ 2015)

Compton Cloud?

Old ('70s) and New problem
- "corona" or "inner region
(2 temperature SLE model)"

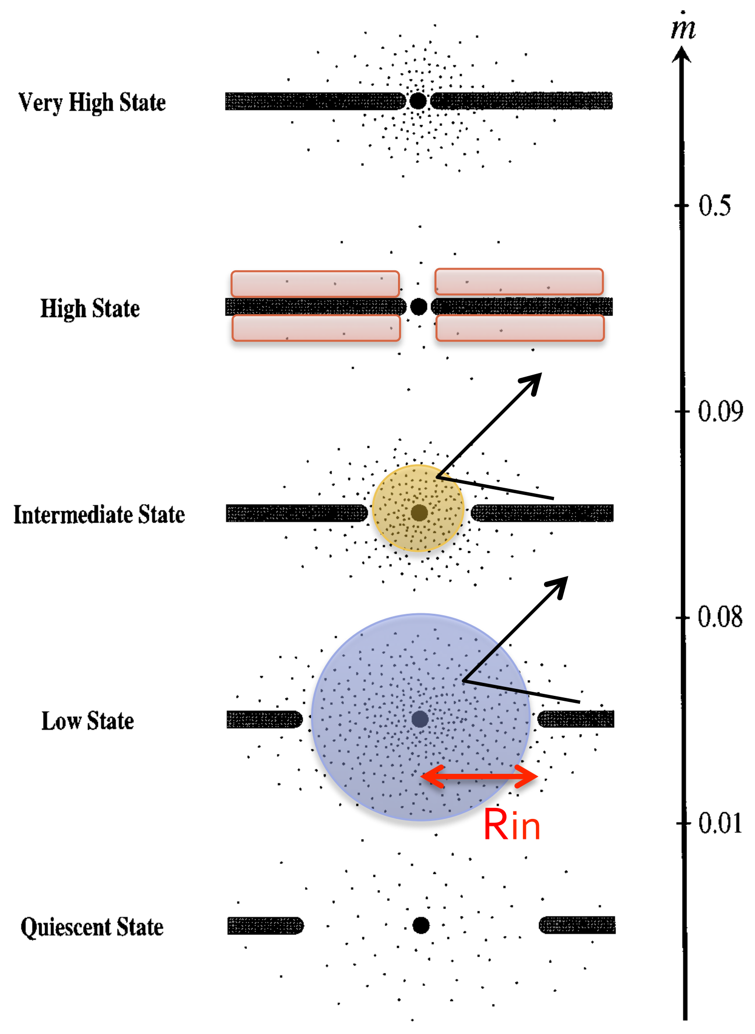

Fitting gives
Electron Temperature: Te, τ (Γ)
Disk parameters: Tbb, Rin
Compton Fraction: fc

if Corona, a real vertical structure?
soft state : Rin <= color temperature correction
Tcolor/Teff ~ 1.7-1.9 (Shimura+ 1995),
~ 1.5-1.6 (e.g., Devis+ 2005)
AND competing with Corona!
hard state: rapid time variations?

Assuming a spherical region, fc ≤ 20% (indep. of Rin)
hard state : fc > 20%
-> simple model N.G.
-> seed photon: synchrotron, brems?, e.g.,ADAF
(or jet!)

Precise models provide..

ADAF

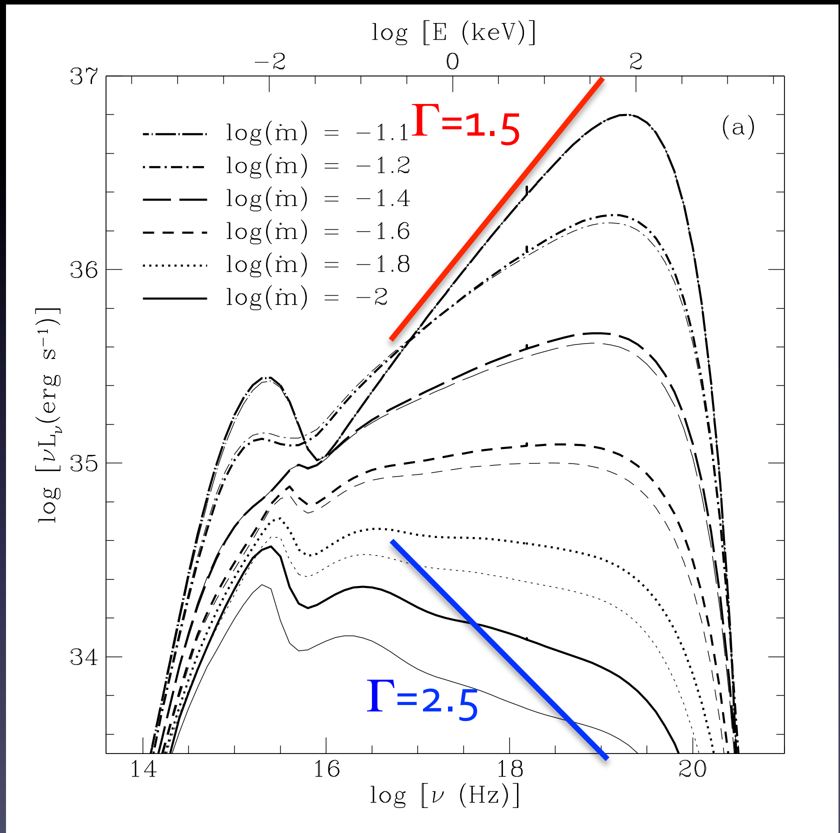

Esin+ 1997

Plasma Pair..

l: compactness parameter

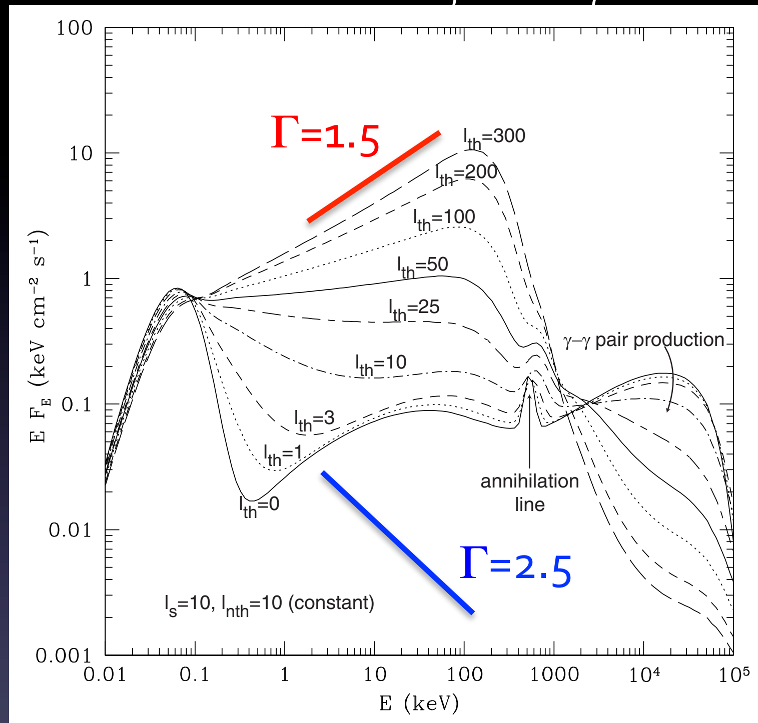

Figure 1. The transition from a non-thermal plasma ($l_{th} = 0$) to a thermally dominated plasma ($l_{th}/l_{nth} = 30$). The soft input into the source has a compactness $l_s = 10$ and has a blackbody spectrum with $T_{bb} = 15$ eV. The assumed source radius is $R = 10^{14}$ cm, and a background plasma is present with optical depth $\tau_p = 0.1$.

Coppi 2002?

観測と一致するようには思えない。。

Soft State

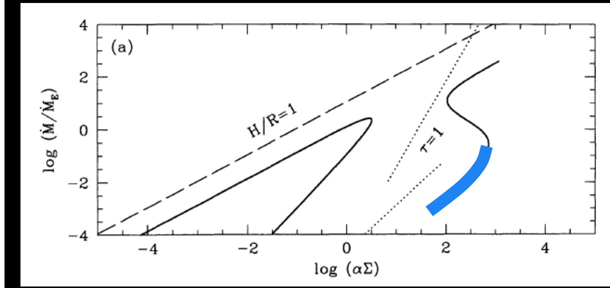

MCD - *Standard Disk*

Shimura & Takahara 1995

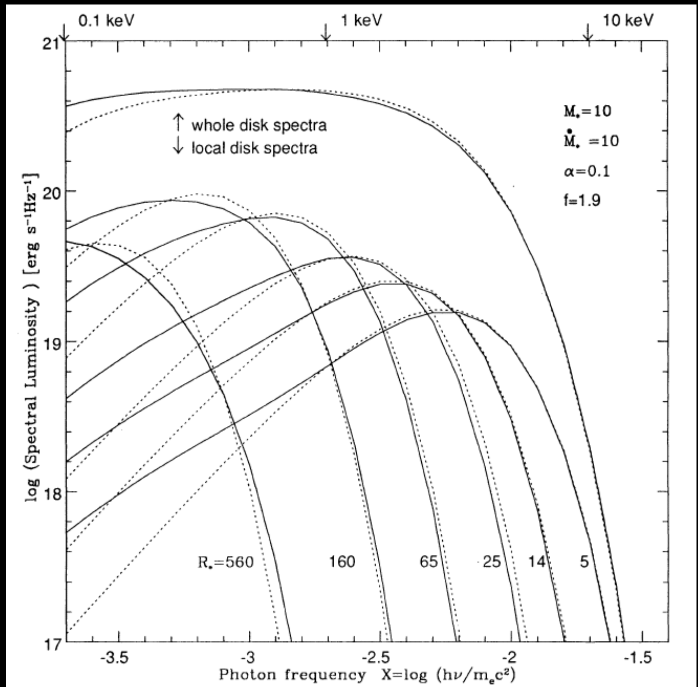

FIG. 1a

ICD) model

Mitsuda et al. 1984

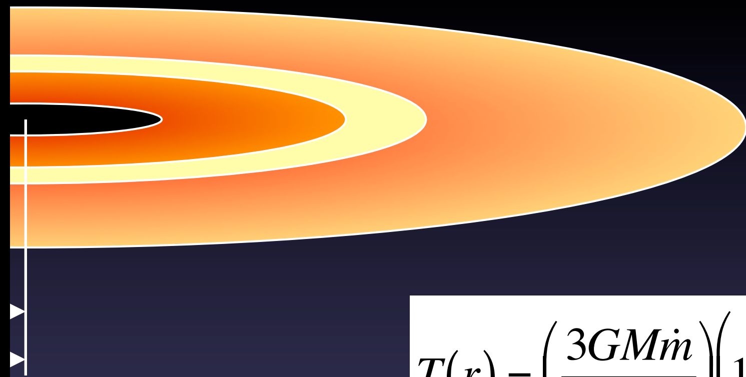

$$T(r) = \left(\frac{3GM\dot{m}}{8\pi\sigma r^3}\right)\left(1 - \sqrt{\frac{r_{in}}{r}}\right)^{1/4}$$

$$T(r) = \left(\frac{GM\dot{m}}{8\pi\sigma r^3}\right)^{1/4} = T_{in}\cdot\left(\frac{r}{r_{in}}\right)^{-3/4}$$

$$f(E) = \frac{\cos i}{d^2}\int_{r_{in}}^{r_{out}} 2\pi r B(E,T(r))dr = \frac{8\pi r_{in}^2 \cos i}{3d^2}\int_{T_{out}}^{T_{in}}\left(\frac{T}{T_{in}}\right)^{-11/3} B(E,T)\frac{dT}{T_{in}}$$

確認された降着円盤の最内縁半径

GX 339-4: *Makishima et al. 1986*

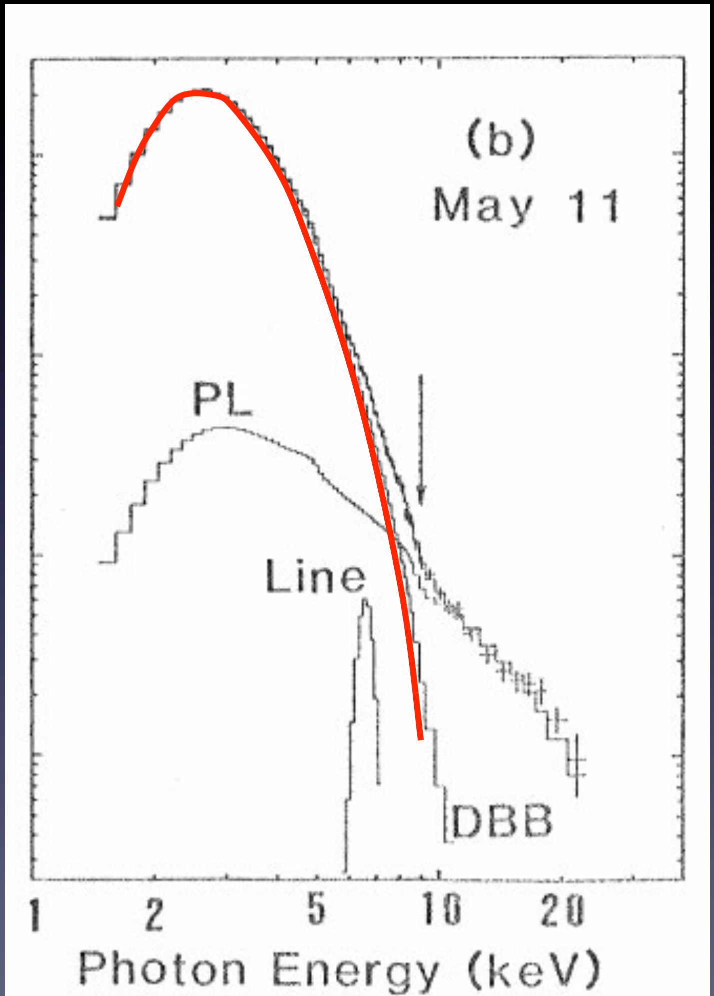

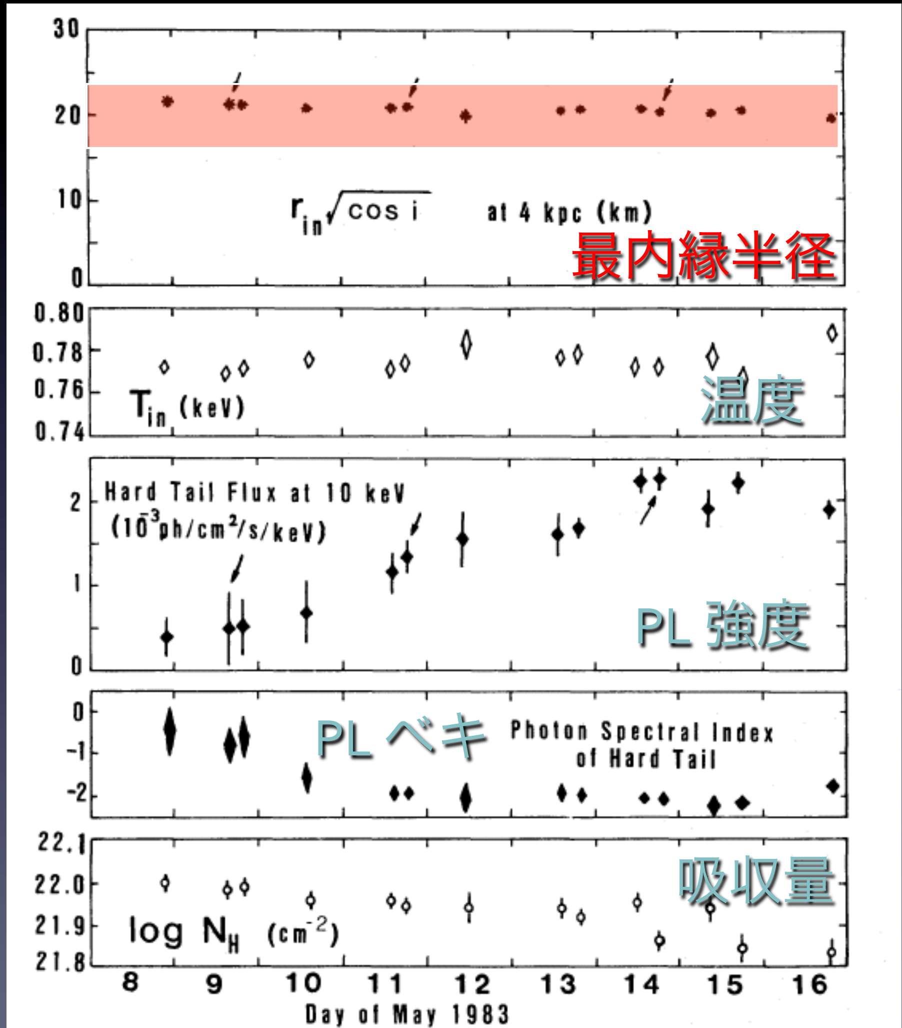

Continuous Spectral Changes
XTE J1752-223

Nakahira+ 2010, PASJ

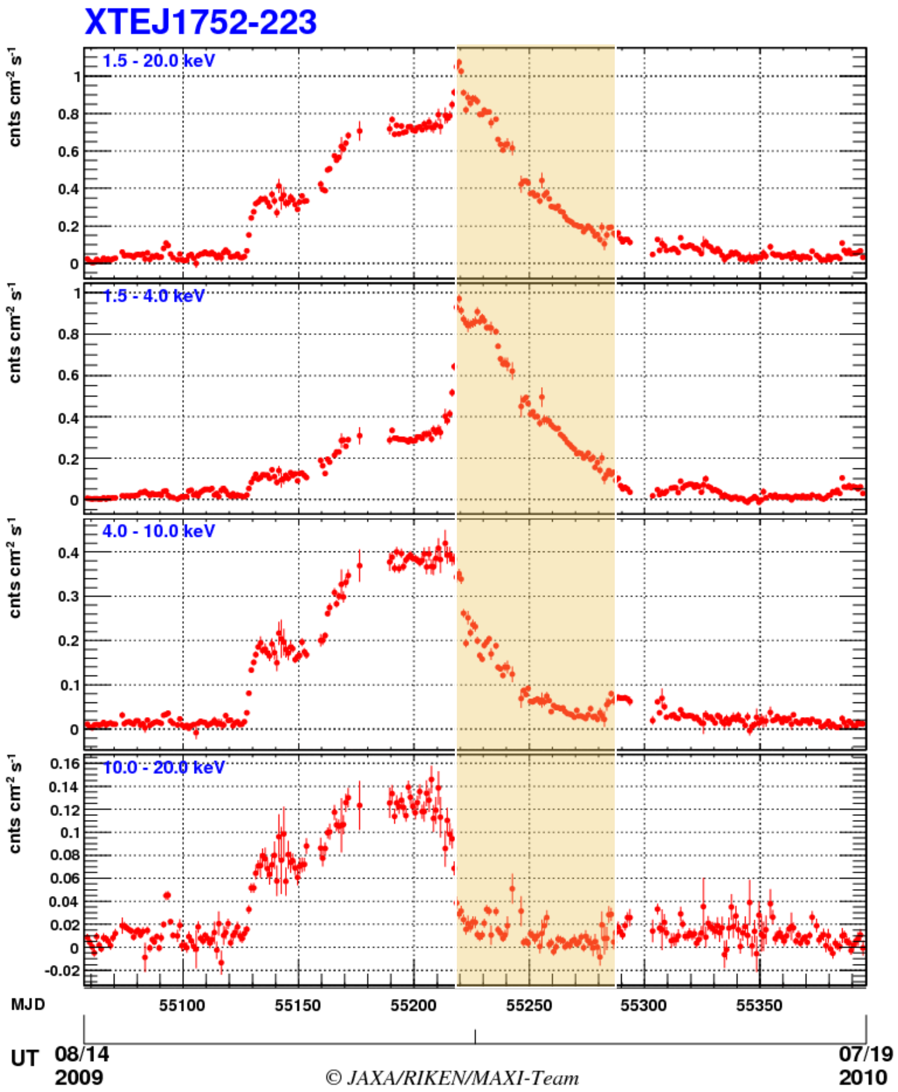

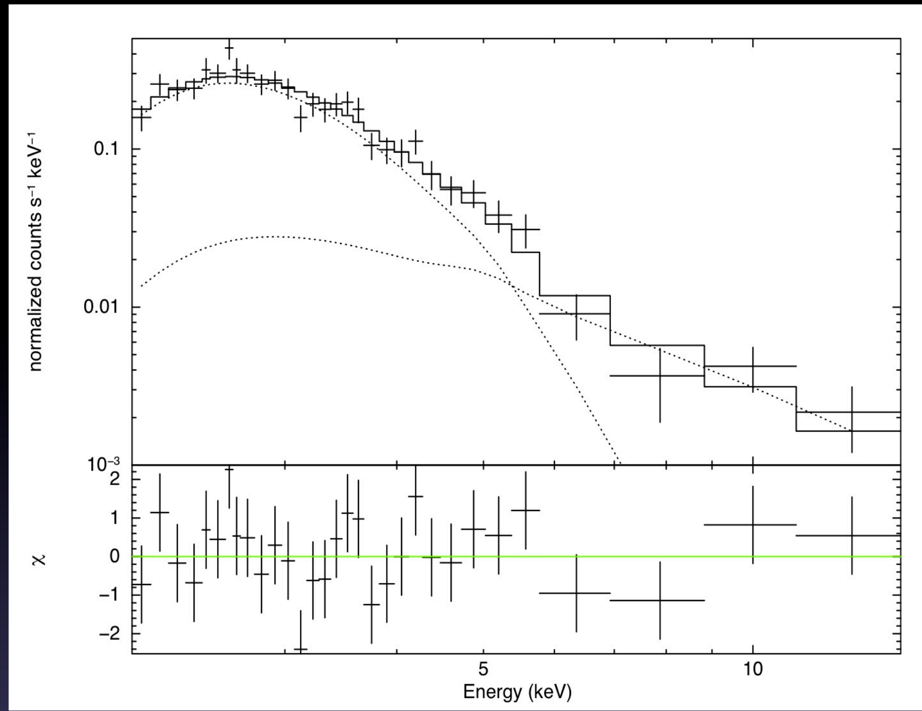

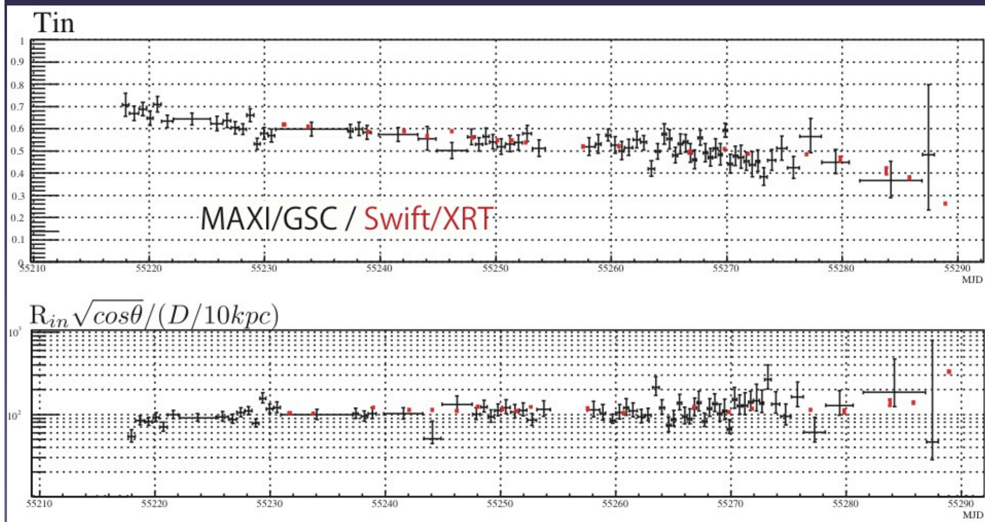

Kerr Spectral models

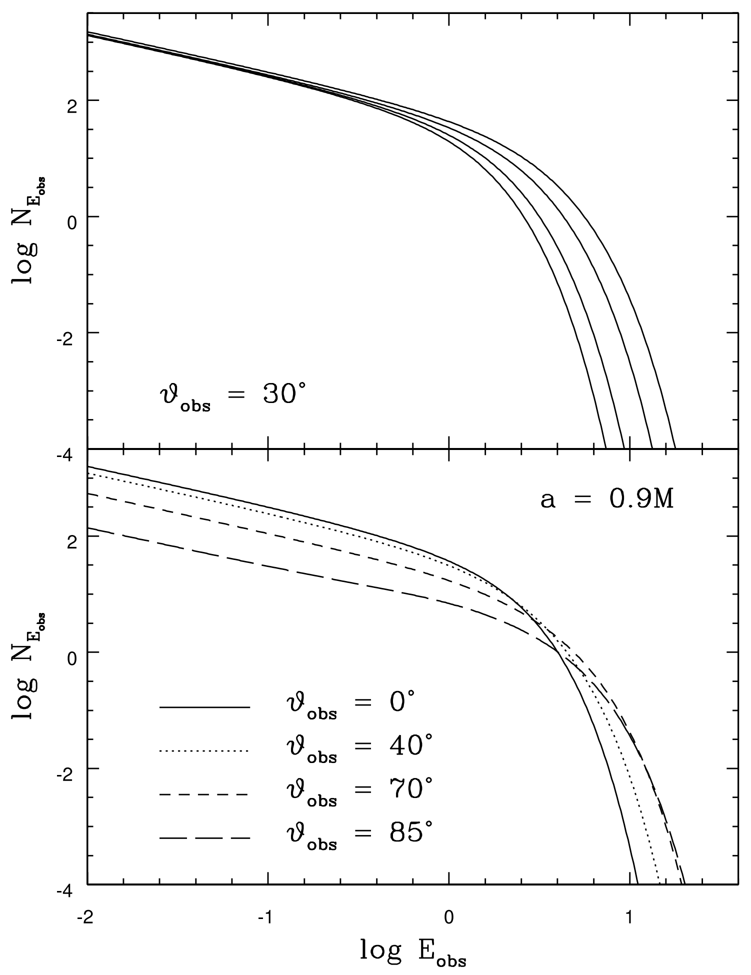

FIG. 5.—*Top*: Effect of the spin of the black hole on the observed spectrum of the disk. From left to right: $a/M = 0, 0.5, 0.9$, and 0.999. Other parameters are $\eta = 0$, $\vartheta_{obs} = 30°$, $M = 10\ M_\odot$, $D = 10$ kpc, $\dot{M} = 10^{19}$ g s^{-1}, and $f_{col} = 1$. *Bottom*: Effect of the inclination angle of the disk on the observed spectrum. The inclination angles are $\vartheta_{obs} = 0°$, 40°, 70°, and 85°, as indicated. Other parameters are $\eta = 0$, $a = 0.9M$, $M = 10\ M_\odot$, $D = 10$ kpc, $\dot{M} = 10^{19}$ g s^{-1}, and $f_{col} = 1$. The energy E_{obs} is in keV, and the flux density $N_{E_{obs}}$ is in units of photons keV^{-1} cm^{-2} s^{-1}.

Li et al. 2005 (kerrbb)

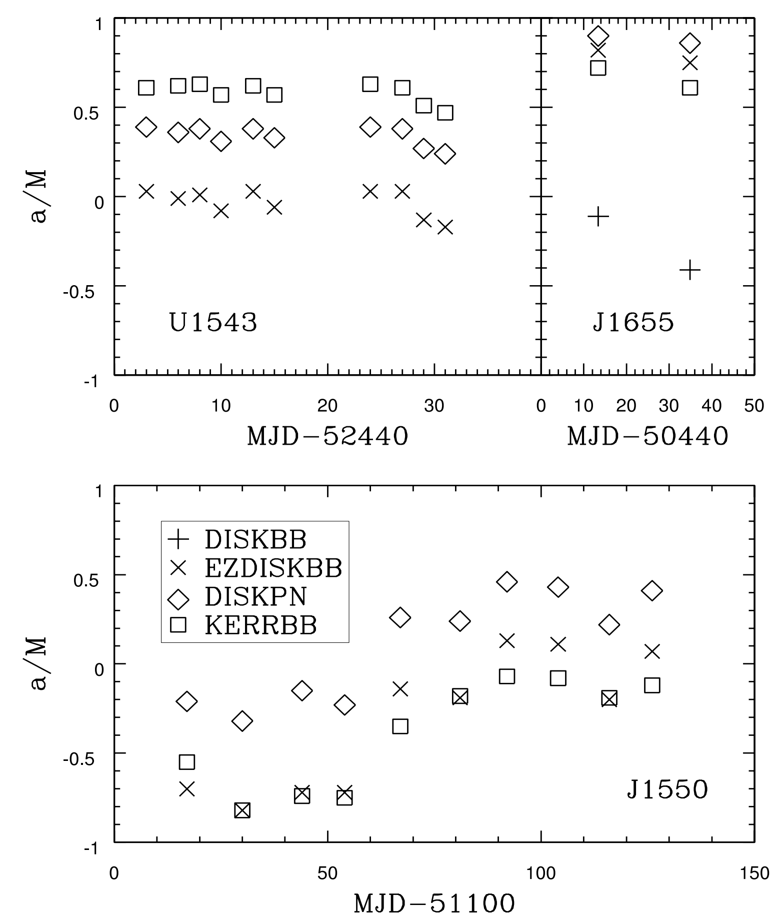

Also, see Davis et al. 2005

Accurate measurements of Rin?

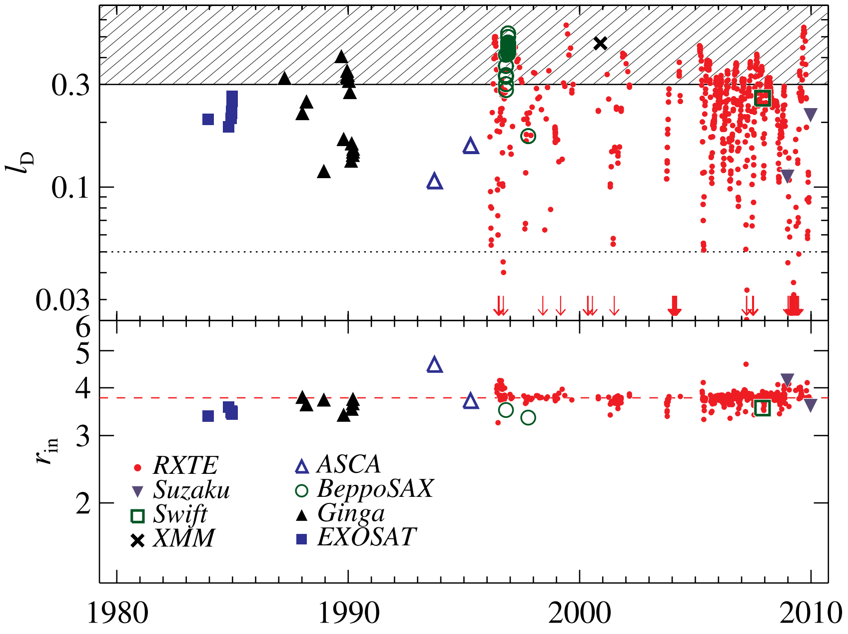

Figure 1. Top: accretion disk luminosity in Eddington-scaled units ($M = 10\ M_\odot$) vs. time for all the data considered in this study (766 spectra). Red arrows show *RXTE* data which are off scale. Data in the unshaded region satisfy our thin-disk selection criterion ($H/R < 0.1$, which implies $l_D < 0.3$; McClintock et al. 2006). The dotted line indicates the lower luminosity threshold (5% L_{Edd}) adopted in Section 3.1. Bottom: values of the dimensionless inner-disk radius r_{in} are shown for thin-disk data in the top panel that meet all of our selection criteria (411 spectra; see Section 3.1). Despite large variations in luminosity, r_{in} remains constant to within ≈4% over time. The median value for the *RXTE* data alone ($r_{in} = 3.77$) is shown as a red dashed line.

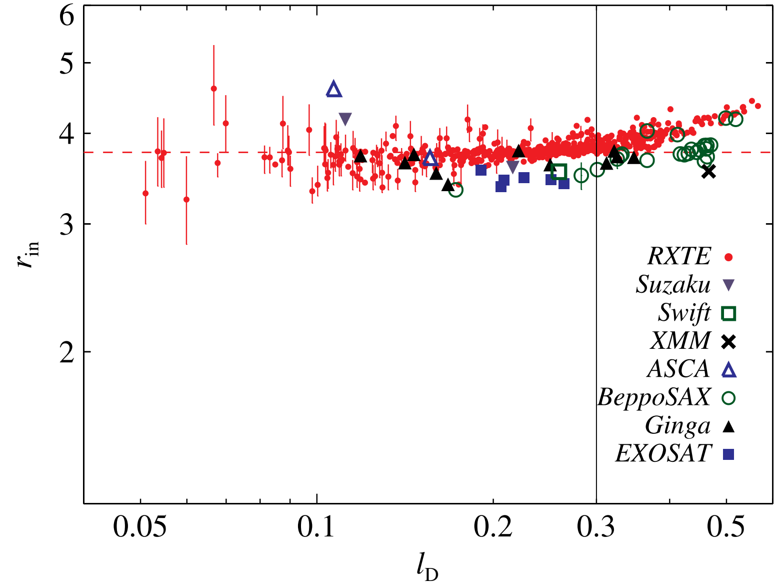

Figure 2. Dimensionless inner-disk radius r_{in} vs. luminosity for the filtered data (Section 3.1) and our baseline model. The vertical black line shows our adopted thin-disk upper limit, $l_D = 0.3$. As in Figure 1, the red dashed line shows the *RXTE* average below this limit.

Steiner+ 2010

cf. Disk Line

Mass and spin : Inner region of the standard disk

simple multi-color disk model: *diskbb* (Mitsuda+ 1984)

+ general relativity: *grad* (Hanawa 1989, Ebisawa+ 1991), *diskpn* (Gierlinski+ 1999)..

+ spin: *kerrbb* (Shafee+ 2006)

+ metal opacities : *bhspec* (Davis+ 2006)

+numerical simulation (Kularni+ 2011)

-> advection, viscos dissipation at risco (radial pressure gradient ?)

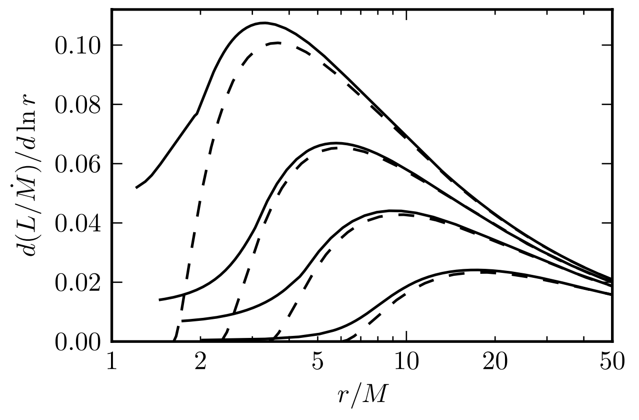

Figure 1. Luminosity profiles from the GRMHD simulations (solid lines) compared with those from the NT model (dashed lines) for $a_* = 0, 0.7, 0.9$ and 0.98 (bottom to top). The disc thicknesses are $|h/r| = 0.05, 0.04, 0.05$ and 0.08 respectively for these runs. The ISCO is located at the radius where the NT disc luminosity goes to zero.

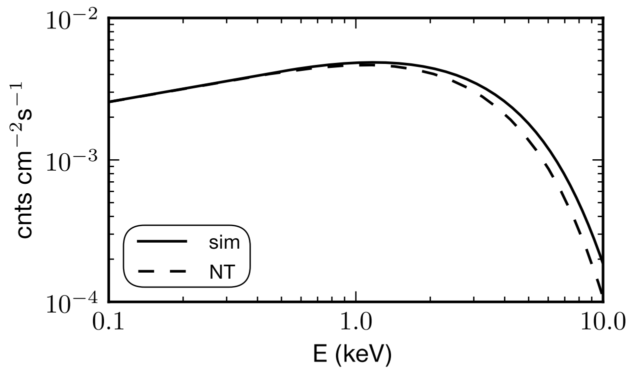

Figure 2. Spectra from the simulated (solid line) and NT (dashed line) discs, for $a_* = 0.9$ and $i = 75°$.

Kulkarni+ 2011

Very High/Intermediate State

Various Types of the LF QPOs in the VH/IM state

XTE J1550-564
Remillard et al. 2002a

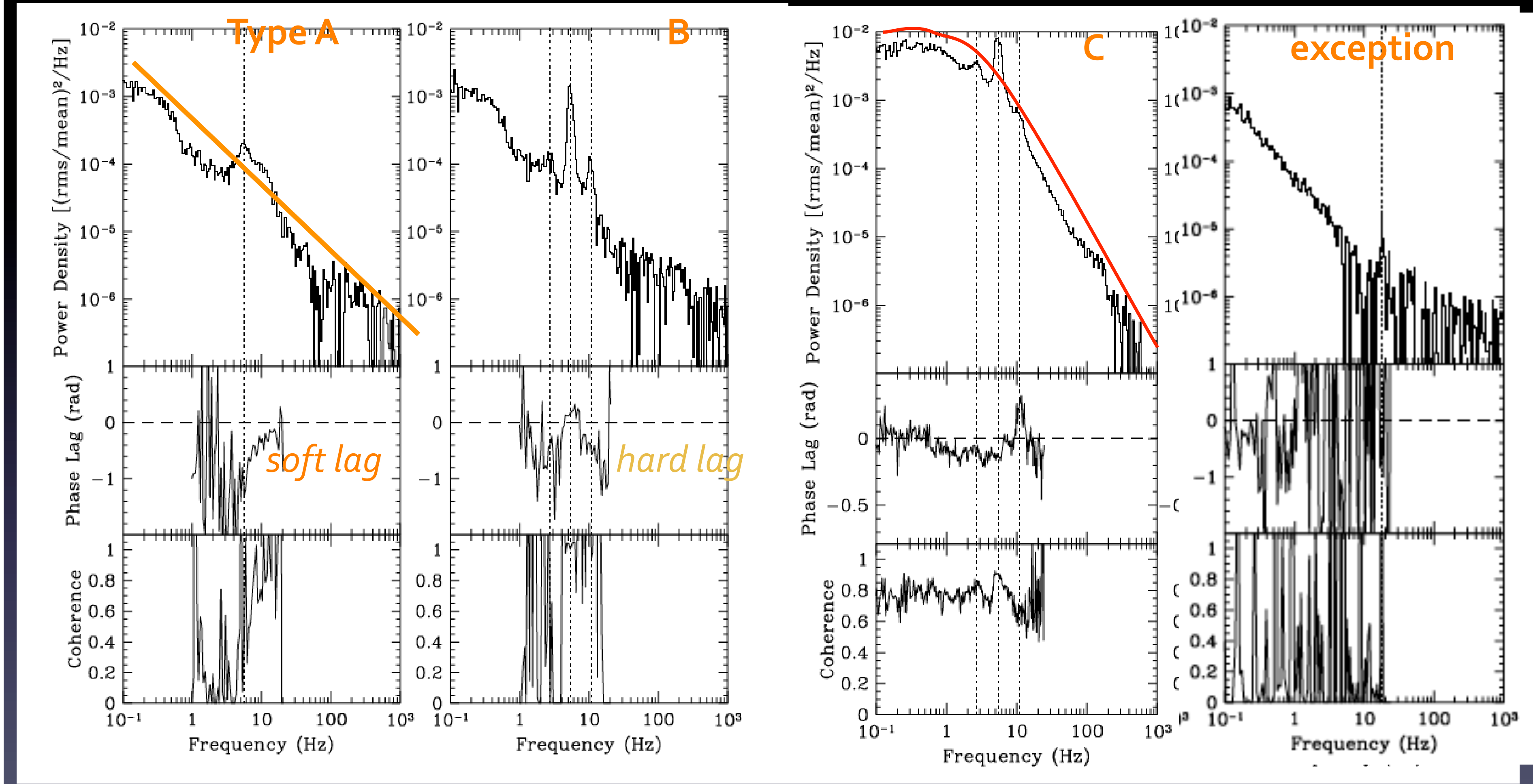

	A	B	C
ν_0	~ 6 Hz	~ 6 Hz	0.1-10 Hz
Q	≤ 3	≥ 6	≥10
rms	3-4%	~4%	3-16 %

GRO J1655-40
Remillard et al. 2002b
XTE J1859+226
Casella et al. 2004

What is the QPOs ?

Periodic, but not perfectly periodic (quasi-periodic oscillations

$$P \propto \frac{\lambda}{(\nu - \nu_0)^2 + (\lambda/2)^2}$$

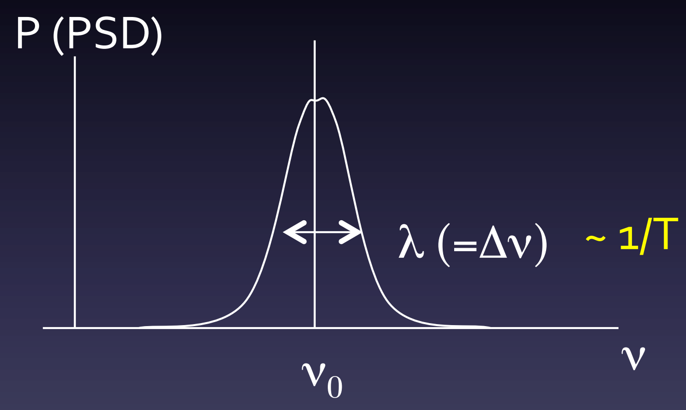

Quality Factor (van der Klis)

$$Q \equiv \frac{\nu_0}{\lambda} \left(= \frac{\nu_0}{\Delta\nu} \right)$$

QPO : (νT >) Q > 2,

If Q ~ νT, then completely periodic
(T: time interval, $\Delta\nu$ T ~ 1)

What makes the QPOs ?

$$x(t) \propto \exp(-t/\tau)\cos(2\pi v_0 t)$$

$$\tau = 1/\pi\lambda$$

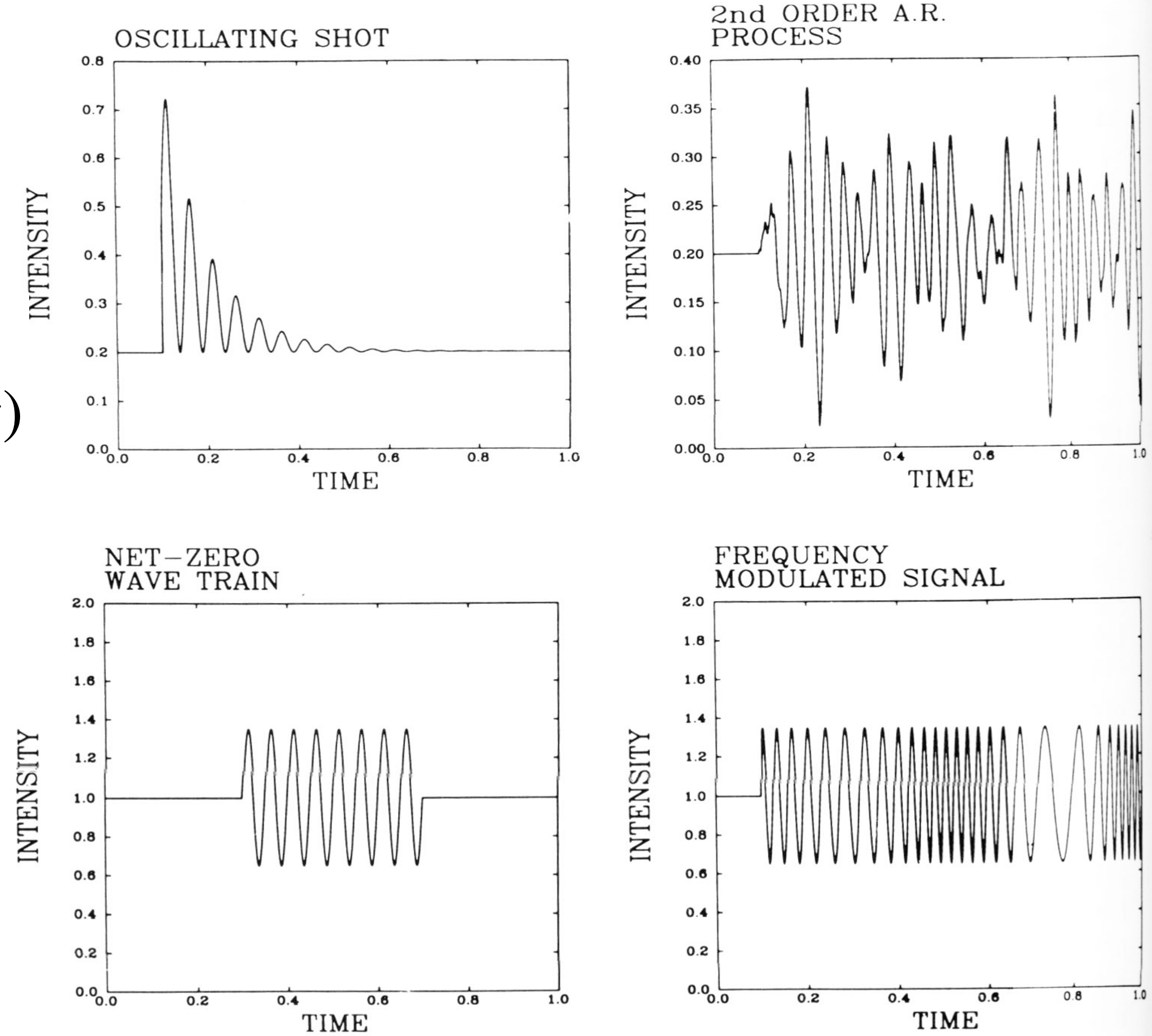

Fig. 6.2. Examples of time series that cause a QPO peak in the power spectrum (Van der Klis 1989b).

van der Klis 1989

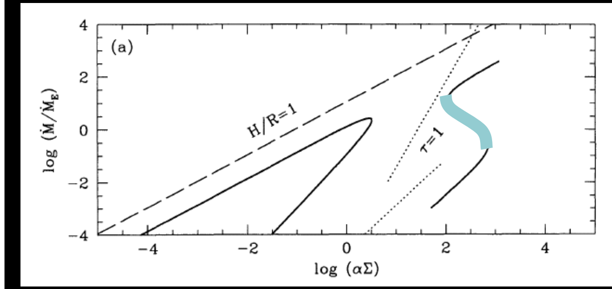

Low frequency Quasi-Periodic Oscillation

Disk Oscillation/LE-instability ?

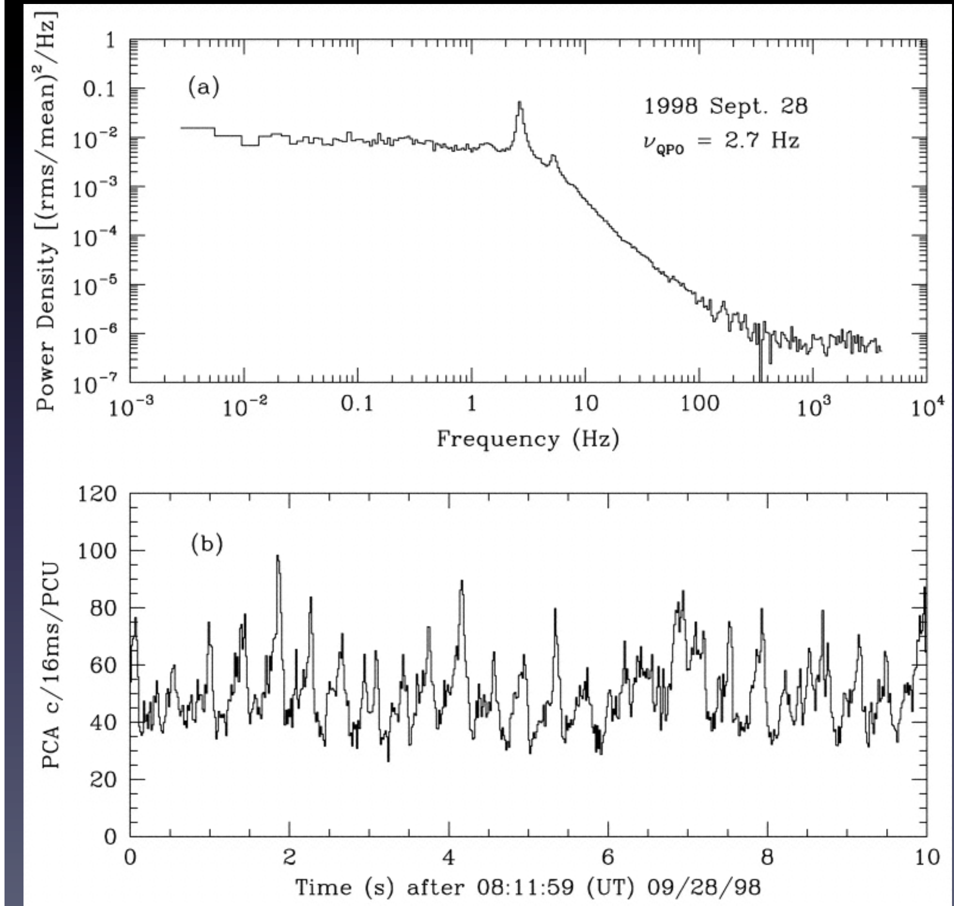

XTE J1550-564/RXTE: *Sobcrak et al. 2002*

(Superposition)

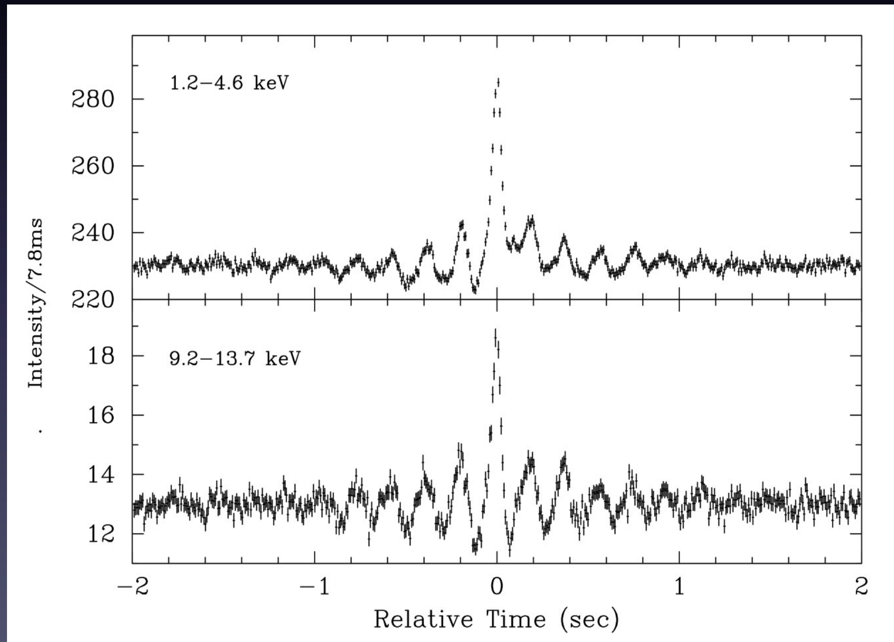

GS 1124-684/Ginga: *Negoro 1997*

HF QPOs

XTE J1550-564
Remillard et al. 2002b

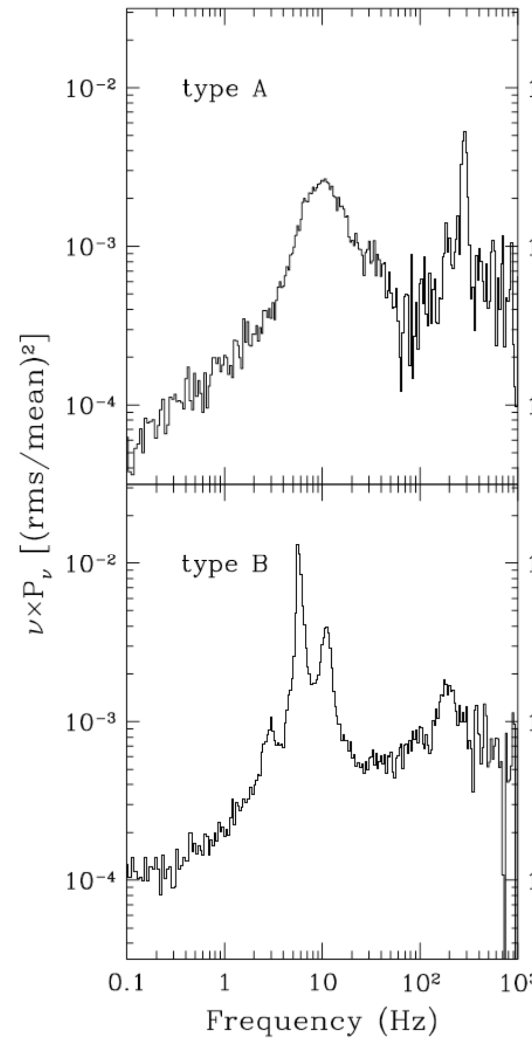

FIG. 1.—Average power spectra for observations of XTE J1550–564 grouped by the type (A, B, or C) of low-frequency QPOs that were observed the 1998–1999 outburst. We also show the PDS for the intense 7 crab flare that was sampled on 1998 September 19.

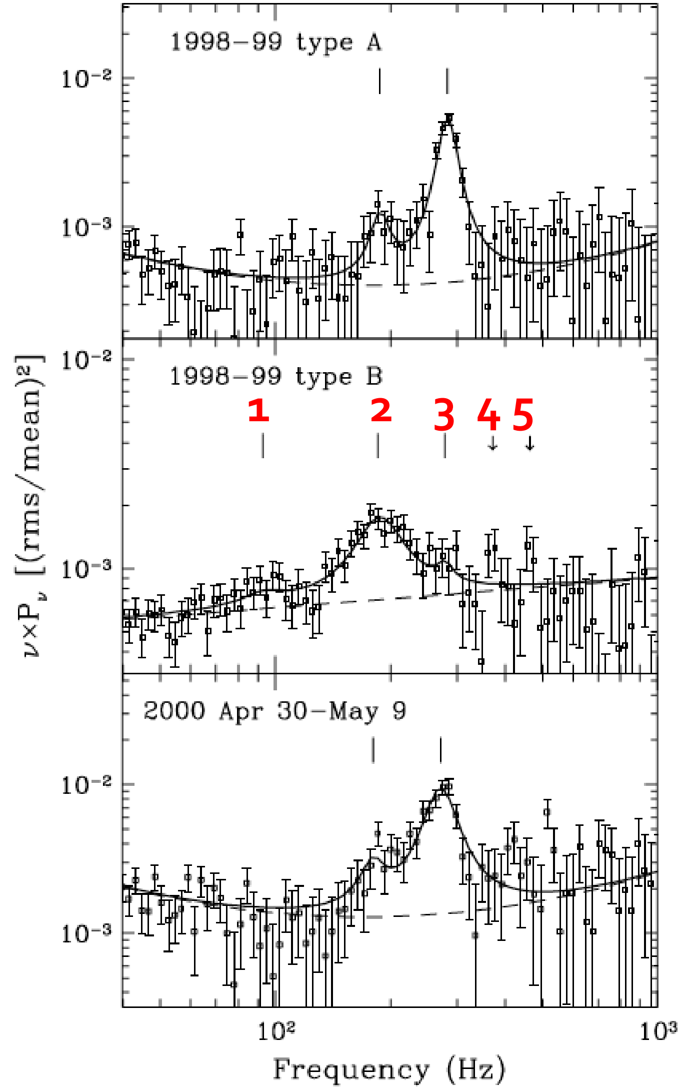

FIG. 2.—Fits for harmonically related HFQPOs in XTE J1550–564 in power spectra at 6–30 keV. The top two panels show the same data displayed in Fig. 1. The bottom panel shows the QPO fit for the average of 12 observations between 2000 April 30 and May 9. In each panel the tick marks above the data show the central frequencies of significant QPOs. The best fit is shown with a smooth, dark curve, and the power continuum is shown with a dashed line. For the type B group (*middle panel*), the arrows show the expected locations of the fourth and fifth harmonics.

HF QPO Stability

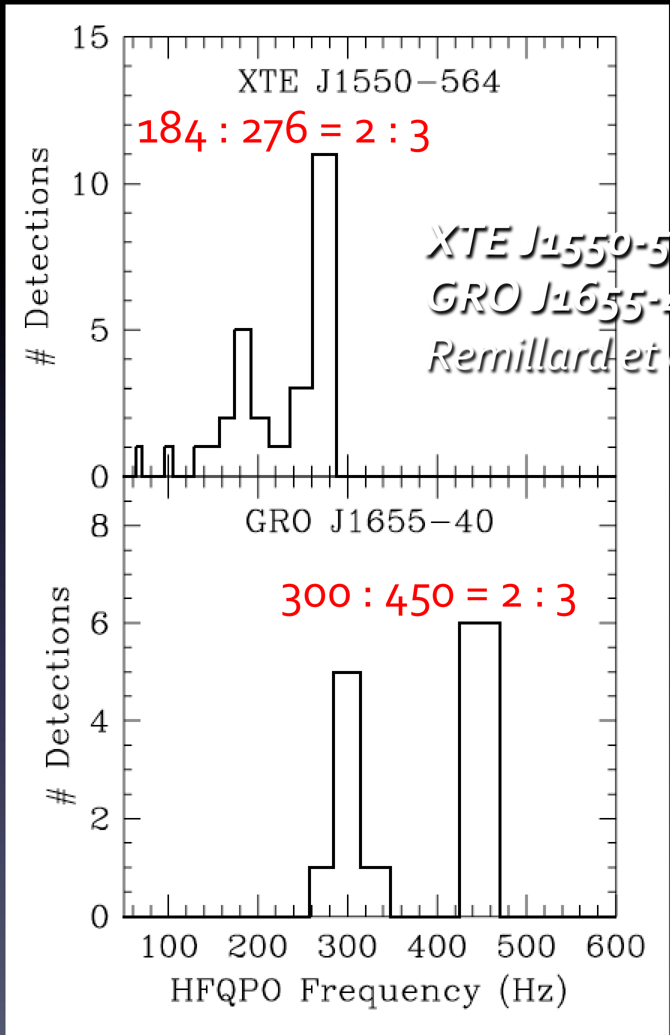

FIG. 3.—Histogram of HFQPO frequencies for XTE J1550−564 and GRO J1655−40. The binning intervals are varied to maintain a width of ±5% relative to the central frequency. Each source displays two peaks in the distribution that have a 3 : 2 ratio in frequency.

XTE J1550-564
GRO J1655-40
Remillard et al. 2002b

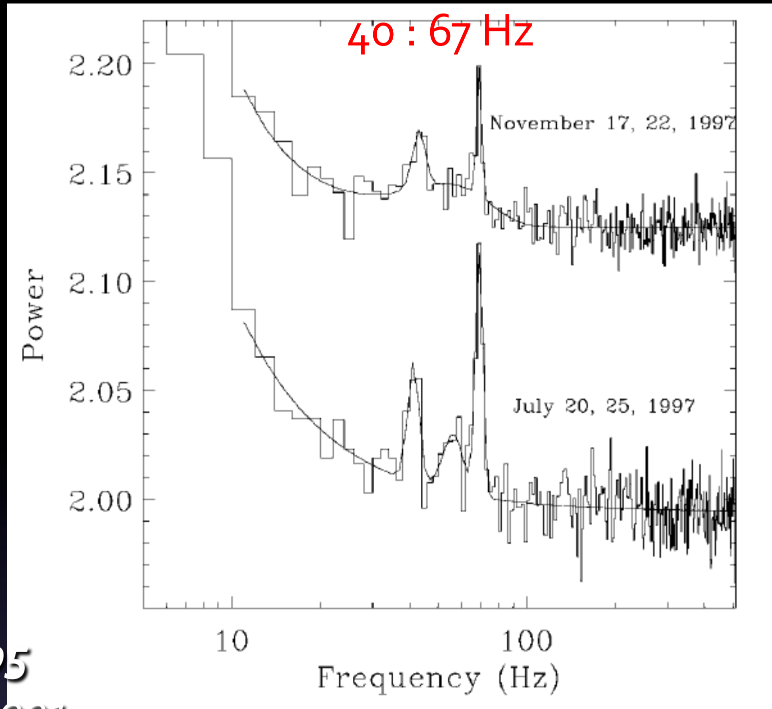

GRS 1915+105
Strohmayer 2001

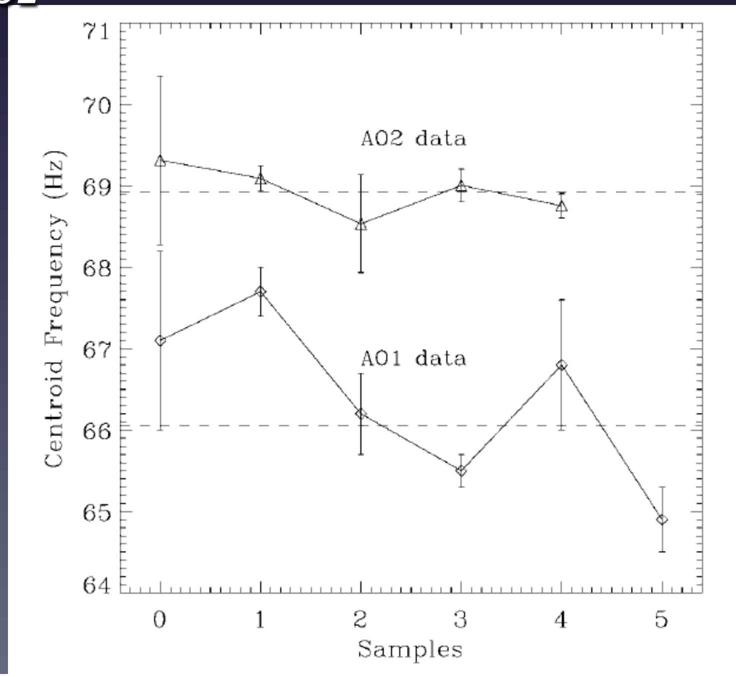

HF QPO Models

(Epicyclic) Resonant disk oscillation : Abramowicz et al. 2004
… by Disk Warps: Kato 2004
(Lense-Thirring: Stella+'98, Ingram+ '09)

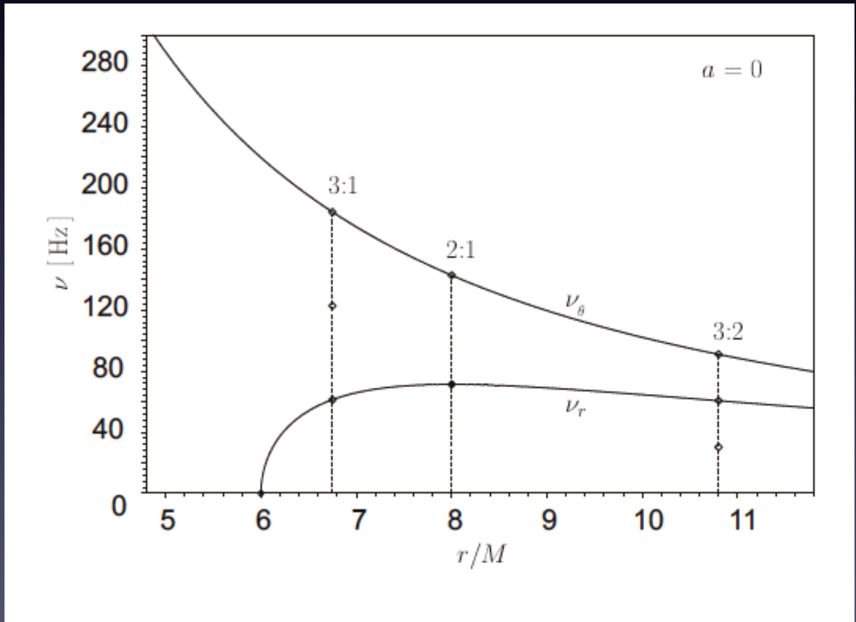

Abramowicz et al. 2004

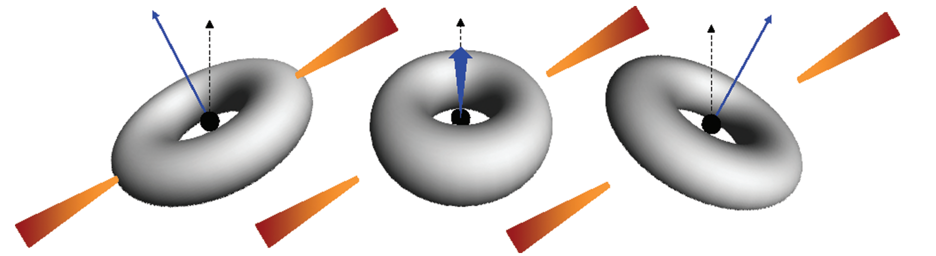

Figure 2. Schematic diagram of the geometry considered. The inner flow (grey with blue angular momentum vector) precesses about the black hole angular momentum vector whilst the outer disc (red/orange) remains aligned with the binary partner. The flow extends between $r_{\rm i}$ and $r_{\rm o}$.

Ingram et al. 2009

BH spin parameters from 2 different methods

from Thermal Spectrum Fits

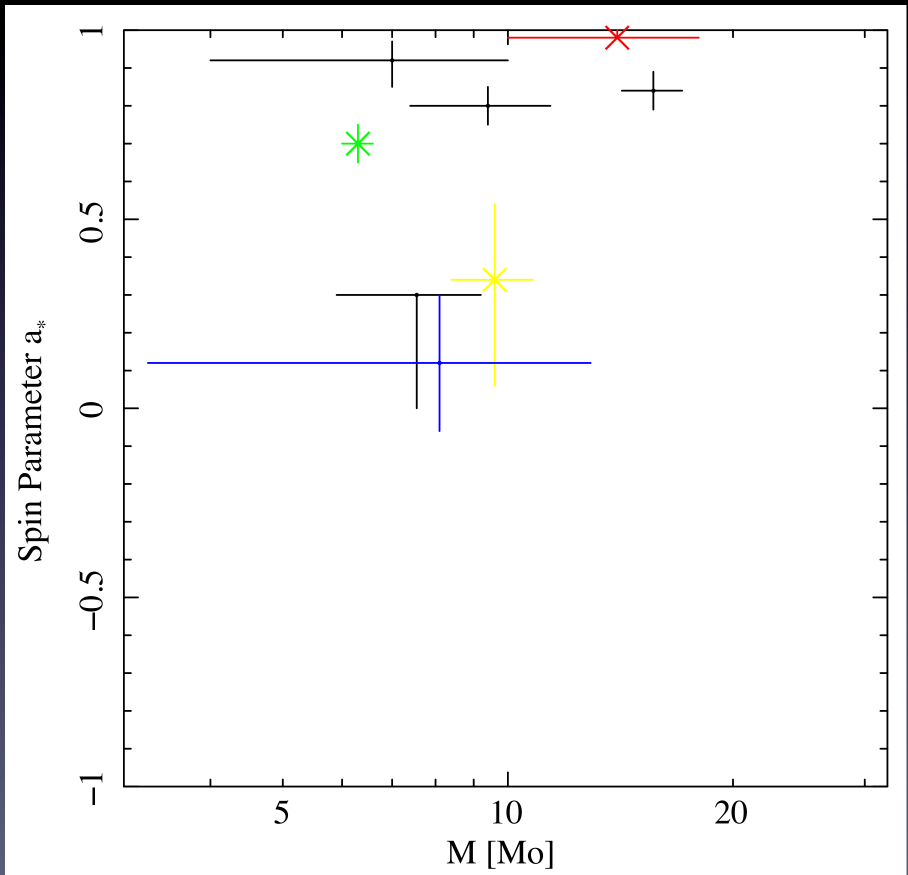

from High Freqeuency -QPOs

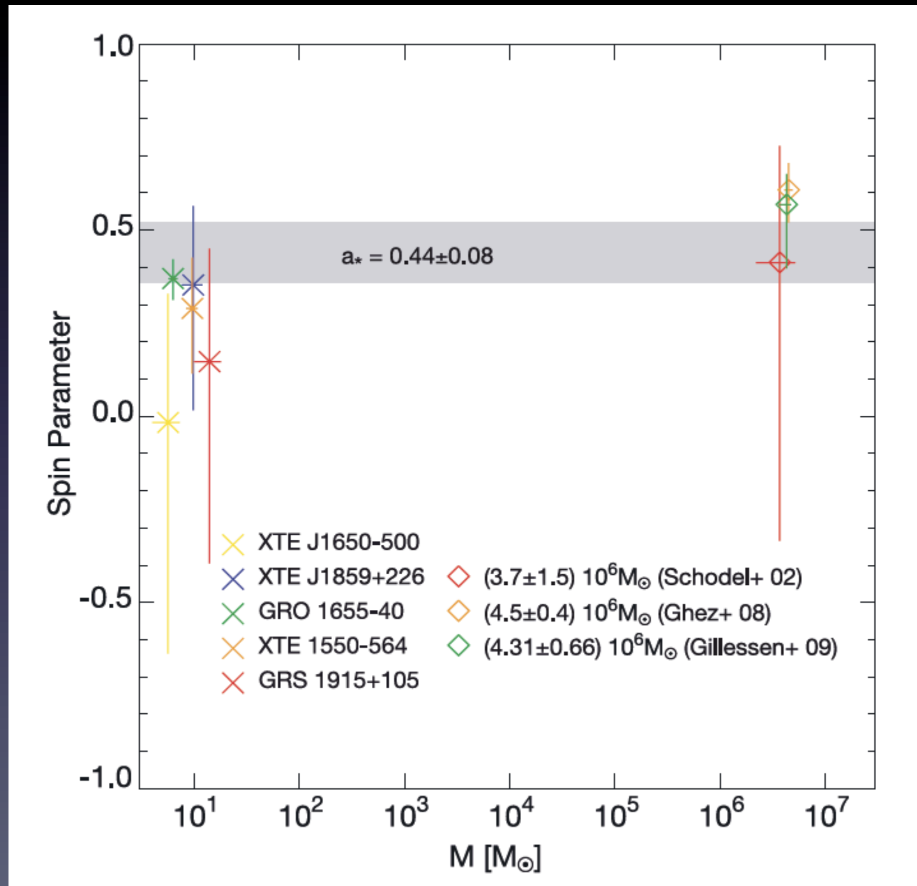

Values are from McClintock et al. 2011

Kato et al. 2010

まとめ

- ブラックホール降着円盤からのスペクトルは（光学的に厚い）熱的円盤成分とべき型成分からなる
- Low/Hard State
  - Shot 後半にジェットが発生 (?)
  - 最内縁付近の情報を持っているはず。Penrose (+) 過程が効く？
- High/Soft State
  - 熱的成分は、相対論、inflow に考慮して、モデル化はかなり進んでいる
    - （質量, 距離が分かれば）スピンも決められる。HF-QPO と一致しない
    - べき成分との関係？そもそもべき成分の起源は？
    - 単純な diskbb モデルとの関係は？ (常に bhspec がベスト?)
  - 鉄輝線
    - 光源の起源、連続成分の寄与、モデル化にまだ不確定性が多い
- IM/VHS
  - Relativistic Jet
  - (Low/High frequency) QPO は理論的にはまだ未解決